Automatica 171 (2025) 111937

Contents lists available at ScienceDirect

Automatica

journal homepage: www.elsevier.com/locate/automatica

Modeling and analysis of a coupled SIS bi-virus model ☆

Sebin Gracy [a,*], Philip E. Paré [b], Ji Liu [c], Henrik Sandberg [d], Carolyn L. Beck [e], Karl Henrik Johansson [d], Tamer Başar [e]

[a] Department of EECS, South Dakota School of Mines and Technology, SD, USA
[b] Elmore Family School of Electrical and Computer Engineering, Purdue University, IN, USA
[c] Department of Electrical and Computer Engineering, Stony Brook University, USA
[d] Division of Decision and Control Systems, School of Electrical Engineering and Computer Science, KTH Royal Institute of Technology, and Digital Futures, Stockholm, Sweden
[e] Coordinated Science Laboratory, University of Illinois at Urbana-Champaign, USA

ARTICLE INFO

Article history:
Received 9 July 2022
Received in revised form 1 July 2023
Accepted 20 August 2024
Available online 25 September 2024

Keywords:
Spreading processes
Epidemics
Coupled bi-virus spread
Stability analysis

ABSTRACT

The paper deals with the setting where two viruses (say virus 1 and virus 2) coexist in a population, and they are not necessarily mutually exclusive, in the sense that infection due to one virus does not preclude the possibility of simultaneous infection due to the other. We develop a coupled bi-virus susceptible–infected–susceptible (SIS) model from a 4^n-state Markov process, where n is the number of agents (i.e., individuals or subpopulation) in the population. We identify a sufficient condition for both viruses to eventually die out, and a sufficient condition for the existence, uniqueness and asymptotic stability of the endemic equilibrium of each virus. We establish a sufficient condition and multiple necessary conditions for local exponential convergence to the boundary equilibrium (i.e., one virus persists, the other one dies out) of each virus. Under mild assumptions on the healing rate, we show that there cannot exist a coexisting equilibrium where for each node there is a nonzero fraction infected only by virus 1; a nonzero fraction infected only by virus 2; but no fraction that is infected by both viruses 1 and 2. Likewise, assuming that healing rates are strictly positive, a coexisting equilibrium where for each node there is a nonzero fraction infected by both viruses 1 and 2, but no fraction is infected only by virus 1 (resp. virus 2) does not exist. Further, we provide a necessary condition for the existence of certain other kinds of coexisting equilibria. We show that, unlike the competitive bivirus model, the coupled bivirus model is not monotone. Finally, we illustrate our theoretical findings using an extensive set of simulations.

1. Introduction

The phenomenon of spreading processes has been a key facet of human civilization. Several manifestations of this phenomenon are witnessed in the present day too, including the spread of opinions in social networks, diseases in contact networks, viruses in computer networks, products in markets, etc. Given the various ramifications of such processes, researchers across diverse disciplines such as physics (Newman, Forrest, & Balthrop, 2002), ecology (Munster & Fouchier, 2009), epidemiology (Bailey et al., 1975), and computer science (Wang, Chakrabarti, Wang, & Faloutsos, 2003) have devoted significant attention to the same.

This paper deals with the spread of viruses in human contact networks. The first model to capture the spread of a virus was proposed by Daniel Bernoulli in the 18th century to calculate the gain in life expectancy at birth if smallpox were to be eliminated as a cause of death (Bernoulli, 1760). As a discipline in its own right, mathematical epidemiology witnessed enormous growth in the 20th century, with (Bailey et al., 1975;

☆ The work of SG and HS was supported in part by the Knut and Alice Wallenberg Foundation, Sweden, Swedish Research Council, Sweden under Grant 2016-00861; and that of KHJ by a Distinguished Professor Grant from the Swedish Research Council, Sweden (Org: JRL, project no: 3058), by the Swedish Strategic Research Foundation SUCCESS Grant FUS21-0026, and by a Knut and Alice Wallenberg Foundation Wallenberg Scholar Grant. The work of PEP was supported by the National Science Foundation, USA, grants NSF-ECCS 2032258 NSF-ECCS 2238388. The work of JL was supported by the Air Force Office of Scientific Research (AFOSR) under award number FA9550-23-1-0175. Joint research of CLB and TB was supported by the National Science Foundation, USA Grant NSF-ECCS 2032321. The material in this paper was partially presented at the 2018 American Control Conference (ACC), June 27–29, 2018, Milwaukee WI, USA. This paper was recommended for publication in revised form by Associate Editor Nima Monshizadeh under the direction of Editor Christos G. Cassandras.

* Corresponding author.
E-mail addresses: sebin.gracy@sdsmt.edu (S. Gracy), philpare@purdue.edu (P.E. Paré), ji.liu@stonybrook.edu (J. Liu), hsan@kth.se (H. Sandberg), beck3@illinois.edu (C.L. Beck), kallej@kth.se (K.H. Johansson), basar1@illinois.edu (T. Başar).

https://doi.org/10.1016/j.automatica.2024.111937

Hethcote, 2000) being some of the key works. One of the fundamental research objectives in mathematical epidemiology is to analyze the system equilibria and determine the convergence behavior of epidemic processes in the vicinity of isolated equilibria. Leveraging such analysis enables the design of mitigation (or eradication) strategies. To this end, various models have been studied in the literature: susceptible–infected–recovered (SIR) (Mei, Mohagheghi, Zampieri, & Bullo, 2017); susceptible–exposed–infected–recovered (SEIR) (Arcede, Caga-Anan, Mentuda, & Mammeri, 2020); susceptible–asymptomatic–infected–recovered susceptible (SAIRS) (Paré, Beck, & Başar, 2020); susceptible–infected (SI) (Matouk, 2020); and susceptible-infected–susceptible (SIS) (Castillo-Chavez, Hethcote, Andreasen, Levin, & Liu, 1989; Khanafer, Başar, & Gharesifard, 2016; Van Mieghem, Omic, & Kooij, 2009) being some of the notable ones.

The focus of this paper is on the susceptible-infected-susceptible (SIS) model. In particular, we are interested in *networked SIS models* Networked SIS models have been extensively studied in the literature; see, for instance, (Fall, Iggidr, Sallet, & Tewa, 2007; Khanafer et al., 2016; Paré, Beck, & Başar, 2020).

Note that none of the aforementioned papers account for settings where multiple strains of a virus could be *simultaneously* active within a population. The dynamics in the multi-virus setting are far richer than those in the single-virus setting. More specifically, suppose that there are two viruses, say virus 1 and virus 2, prevalent; then these viruses could be either (a) competitive, e.g., leprosy and tuberculosis (Castillo-Chavez et al., 1989; Sahneh & Scoglio, 2014; Zhang, Gracy, Başar, & Paré, 2022); or (b) co-operative, e.g., human immunodeficiency virus (HIV) and syphilis (resp. herpes simplex virus type 2 (HSV-2)) (Beutel, Prakash, Rosenfeld, & Faloutsos, 2012; Xu, Lu, & Zhan, 2012; Zhao, Wang, & Ruan, 2020). In the competitive regime, an agent can be infected either with virus 1 or with virus 2 or neither, whereas in the co-operative regime (also referred to as co-infection) an agent can be *simultaneously* infected with both virus 1 and virus 2.

Bi-virus models that capture the possibility of an agent being infected with more than one virus at the same time are broadly referred to as *coupled bi-virus models*. Such scenarios are extremely common during pandemics. In fact, during the Covid-19 pandemic, there were reports of coinfections with SARS-Cov-2 and influenza A virus (Wang et al., 2020), while a 90-year old woman in Belgium was simultaneously infected with both the alpha and beta variants of SARS-Cov-2 (Roberts, 2021). In a similar vein, co-infections with Zika and Dengue viruses have also been reported in the past (Dupont-Rouzeyrol et al., 2015). Other examples include individuals being simultaneously infected with both tuberculosis and human immunodeficiency virus (HIV), and such coinfections pose particular challenges both from therapeutical and diagnostic perspectives (Pawlowski, Jansson, Sköld, Rottenberg, & Källenius, 2012); with HIV and malaria (Alemu, Shiferaw, Addis, Mathewos, & Birhan, 2013); with Hepatitis B and C (Chu & Lee, 2008); and with chlamydia and gonorrhea (Creighton, Tenant-Flowers, Taylor, Miller, & Low, 2003). The phenomenon of coinfection is also observed in animals; some examples include coinfection with different strains of foot-and-mouth disease virus in livestock (Arzt et al., 2021); with H9N2 and H7N9 avian influenza viruses in poultry (Bhat et al., 2022); and with different subtypes of the Hepatitis E virus in swine (de Souza et al., 2012).

In this paper, our focus is on the development and analysis of a coupled networked SIS bi-virus model. The authors in (Beutel et al., 2012) proposed such a model, but it accounted only for undirected graphs, and each of the nodes are restricted to have the same healing and infection rates with respect to each of the viruses. A probabilistic coupled bi-virus SIS model was proposed and studied in (Xu et al., 2012), but the authors treated infection and recovery from each virus as probabilities, which implies that those are constrained to stay between zero and one. Differently from (Xu et al., 2012), the model we propose admits nonnegative infection rates and positive healing rates larger than one for each virus. Moreover, we provide a richer analysis of the various equilibria of the co-operative viruses regime. Recently, a coupled bi-virus SIS model that accounts for only a *single* population node has been proposed in (Zhao et al., 2020). Overcoming this limitation, the coupled bi-virus model that we propose admits an arbitrary but finite number of population nodes. The two viruses may spread through possibly different directed contact graphs. An agent could be either infected by virus 1 or by virus 2 or, at the same time, by both (i.e., viruses 1 and 2) or by neither. To better capture the possibilities with respect to simultaneous infection by both viruses 1 and 2, we introduce a coupling parameter $\epsilon^{(m)}$ (≥ 0), where $m = 1, 2$. Specifically, if $\epsilon^{(m)} > 1$ for $m = 1, 2$ then infection with virus 1 (resp. virus 2) increases the possibility of infection with virus 2 (resp. virus 1). Such a scenario is observed with respect to infection with human immunodeficiency virus (HIV) and syphilis (resp. herpes simplex virus type 2 (HSV-2)) (Chen, Ghanbarnejad, Cai, & Grassberger, 2013; Newman & Ferrario, 2013). Similarly, if $\epsilon^{(1)} > 1$ and $\epsilon^{(2)} < 1$ then infection with virus 2 increases the possibility of simultaneous infection with virus 1, but infection with virus 1 decreases the possibility of simultaneous infection with virus 2, e.g., the spread of malicious pathogens and growth of immune cells in living organisms (Ahn, Jeong, Masuda, & Noh, 2006). Likewise, if $\epsilon^{(m)} < 1$ for $m = 1, 2$, then infection with virus 1 (resp. virus 2) decreases the possibility of infection with virus 2 (resp. virus 1). Such a scenario corresponds to the simultaneous circulation of multiple strains of influenza viruses in a community, where the presence of the strain from a previous year(s) (resp. the current year) decreases the possibility of also being simultaneously infected with the strain from the current year (resp. previous years) (Krauland, Galloway, Raviotta, Zimmerman, & Roberts, 2022). We classify the equilibria into the following classes: (a) the healthy state (both viruses are eradicated), (b) single-virus endemic equilibrium (the endemic equilibrium corresponding to that of virus 1 (resp. virus 2) if only virus 1 (resp. virus 2) were prevalent in the population), (c) boundary equilibria (one virus is eradicated, the other one is persistent, fraction of population infected by both is zero), and (d) coexisting equilibria (both viruses simultaneously infect possibly same fractions of the population). It turns out that our model generalizes the competitive networked bi-virus model; see Remark 1.

A particular class of nonlinear systems is *monotone dynamical systems*. Very briefly, a nonlinear system $\dot{x} = f(x)$ is monotone, if, for two initial states x_0 and y_0, $x_0 \leq y_0$ implies $x(t) \leq y(t)$ for all $t \in \mathbb{R}_+$. It is well known that monotone systems, assuming they generically have a finite number of equilibria, converge to a stable equilibrium point (assuming one exists) for almost all choices of system parameters, and that any limit cycle (if it exists) is non-attractive; see (Hirsch, 1988; Smith, 1988)[1]. In the context of epidemiology, the notion of monotone dynamical systems plays a key role in the following sense: supposing that the model governing the spread of a disease is monotone and that it has a finite number of equilibria, then the typical behavior that a policymaker will have to contend with is that of convergence to some equilibrium point (disease-free, endemic, coexistence, etc.). More pertinently, it says that existence of limit cycles (i.e., the occurrence of waves of epidemic) is less likely. Furthermore, even if a limit cycle were to exist, it would be non-attractive (Ye, Anderson, & Liu, 2022). More complicated behavior such as chaos

[1] The term "generically" is to be understood as follows: the choices of system parameters for which convergence to a stable equilibrium does not happen *lies on a set of measure zero.*

could be definitively ruled out (Sontag, 2007). On the contrary, if the system is not monotone, then no dynamical behavior, including chaos, can be definitively ruled out without additional analysis (Sontag, 2007). Note that the competitive bi-virus model is monotone (Ye et al., 2022). However, it is not known if the coupled bi-virus model is monotone.

Our main contributions in this paper are as follows:

(i) We derive the coupled bi-virus model starting with a 4^n-state Markov process; see Eqs. (8)–(10) in Section 2.
(ii) We provide a sufficient condition which ensures that, irrespective of the initial state of the network (i.e., healthy or sick), both viruses eventually die out; see Theorem 1.
(iii) We provide a sufficient condition for the existence, uniqueness, and asymptotic stability of a single-virus endemic equilibrium; see Theorem 2.
(iv) We identify a sufficient condition for local exponential stability of the boundary equilibria (i.e., one virus persists, and the other one dies out); see Theorem 3.
(v) We show that the coupled bi-virus model is not monotone; see Theorem 4. Consequently, one cannot use the existing tools in the literature on competitive bivirus systems, which are deeply rooted in monotone dynamical systems (see Hirsch 1988, Smith 1988), to study the limiting behavior of our model.

Additionally, we provide a necessary and sufficient condition for the healthy state to be the unique equilibrium of the system; see Corollary 1. Assuming both viruses pervade the network, we establish a lower bound on the number of equilibria for the coupled bi-virus system; see Corollary 2. We identify multiple necessary conditions for local exponential convergence to the boundary equilibria; see Proposition 2. Assuming that the healing rates are strictly positive, we show that a point in the $3n$-dimensional state space, where for each node there is a nonzero fraction infected only by virus 1 (resp. virus 2) but no fraction that is infected by both viruses 1 and 2, *cannot* be an equilibrium point; see Proposition 3. Likewise, under mild assumptions on the healing rates, a point, where for each node there is a nonzero fraction infected by both viruses 1 and 2, but no fraction is infected only by virus 1 (resp. virus 2), *cannot* be an equilibrium; see Proposition 4. We establish a necessary condition for the existence of a coexisting equilibrium wherein the fraction of each node infected by only virus 2 is zero and the rest (i.e., the fraction infected by only virus 1 and the fraction infected by both viruses 1 and 2) are strictly positive; see Proposition 5. Finally, we identify a condition that rules out a *given* point in the state space as a coexisting equilibrium where each node has (i) a fraction that is infected only by virus 1; (ii) a fraction that is infected only by virus 2; and (iii) a fraction that is infected by both viruses 1 and 2, see Proposition 6.

Some of the material in this paper was partially presented earlier in an American Control Conference (ACC) paper (Paré, Liu, Beck, & Başar, 2018); the present paper provides a more comprehensive treatment of the work, and considers a more general model. Specifically, the paper provides:

(i) an expansion of the model to the case of virus-dependent coupling parameters that can be greater than 1. However, most of our findings rely on the assumption that $\epsilon^{(m)} \in [0, 1]$ for $m = 1, 2$;
(ii) complete proofs of all the results;
(iii) a derivation of the coupled bi-virus model from a 4^n-state Markov process; see Section 2;
(iv) stability results for the boundary equilibria; see Theorem 3;
(v) existence results for coexisting equilibria; see Propositions 3, 4, 5 and 6.
(vi) a result establishing that the coupled bivirus system is not monotone; see Theorem 4; and
(vii) additional illustrative simulations in Section 8, none of which were included in (Paré et al., 2018).

The paper is organized as follows. The derivation of the coupled bi-virus model from a 4^n-state Markov process is provided in Section 2. The problems of interest and standing assumptions are formally stated in Section 3. The main results for the model developed in Section 2 are split across the next four sections: analysis of the disease-free equilibrium (DFE) is given in Section 4; persistence of a virus in the population is given in Section 5; analysis of various coexisting equilibria are provided in Section 6; and non-monotonicity of the coupled bivirus model is shown in Section 7. The theoretical findings are illustrated in Section 8. A summary of the results of the paper, and some questions of possible interest to the wider community are given in Section 9.

We conclude this section by introducing all the notations to be used in the rest of the paper.

Notation: For any positive integer n, we use $[n]$ to denote the set $\{1, 2, \ldots, n\}$. We use $\mathbf{0}$ and $\mathbf{1}$ to denote the vectors whose entries all equal 0 and 1, respectively, and I to denote the identity matrix, while the dimensions of the vectors and matrices can be inferred from the context. For any vector $x \in \mathbb{R}^n$, we use $x^\top$ to denote its transpose and $\mathrm{diag}(x)$ or X to denote the $n \times n$ diagonal matrix whose ith diagonal entry equals x_i. The notation $1_{a=b}$ is used as an indicator function which takes the value one if a equals b; and zero otherwise. For $1_{A=b}$, where A is a matrix, the result is a binary matrix of the same dimensions as A with entries $1_{a_{ij}=b}$. For any two sets $\mathcal{A}$ and $\mathcal{B}$, we use $\mathcal{A} \setminus \mathcal{B}$ to denote the set of elements in $\mathcal{A}$ but not in $\mathcal{B}$. For any two real vectors $a, b \in \mathbb{R}^n$, we write $a \geq b$ if $a_i \geq b_i$ for all $i \in [n]$, $a > b$ if $a \geq b$ and $a \neq b$, and $a \gg b$ if $a_i > b_i$ for all $i \in [n]$. Likewise, for any two real matrices $A, B \in \mathbb{R}^{n_1 \times n_2}$, we write $A \geq B$ if $A_{ij} \geq B_{ij}$ for all $i \in [n_1]$, $j \in [n_2]$, and $A > B$ if $A \geq B$ and $A \neq B$. For a real square matrix M, we use $s(M)$ to denote the largest real part among the eigenvalues of M, and $\rho(M)$ to denote the spectral radius, i.e., $\rho(M) = \max\{|\lambda| : \lambda \in \sigma(M)\}$, where $\sigma(M)$ denotes the spectrum of M.

A real square matrix A is said to be Metzler if all of its off-diagonal entries are nonnegative. A real square matrix A is said to be a Z-matrix if all of its off-diagonal entries are nonpositive. A Z-matrix is an M-matrix if all its eigenvalues have nonnegative real parts. Furthermore, if an M-matrix has an eigenvalue at the origin, then we say that it is singular; if each of its eigenvalues have strictly positive parts, then we say that it is nonsingular.

2. The model

Consider two viruses spreading over a network of n agents. Each agent may be infected with either or both viruses at the same time. Specifically, each agent can be infected if one of its neighbors is infected. The neighbor relationships among the n agents[2] are described by an n-vertex directed graph. A directed edge from node j to node i means that agent i can be infected by agent j, i.e., agent j is a neighbor of agent i. We use $\mathcal{N}_i$ to denote the set of neighbors of agent i. The two viruses may spread through different routes in the network. We use $\mathcal{N}_i^{(m)}$ to denote the set of neighbors of agent i from which virus m spreads, $m \in \{1, 2\}$. Clearly, $\mathcal{N}_i^{(1)} \cup \mathcal{N}_i^{(2)} = \mathcal{N}_i$ for all $i \in [n]$.

For each virus $m \in \{1, 2\}$, each agent i has its curing rate $\delta_i^{(m)}$ and infection rates $\beta_{ji}^{(m)}$ when $i \in \mathcal{N}_j^{(m)}$. The former means that if agent i is infected by virus m, it is cured with rate $\delta_i^{(m)}$, and the

[2] Throughout this paper, the terms agents and nodes are used interchangeably.

latter means that if agent i is infected by virus m and its neighbor j is not, agent i can infect agent j at rate $\beta_{ji}^{(m)}$. The two viruses can simultaneously infect the same node, but not independently. Specifically, they are coupled in the following manner. Let i and j be any pair of integers in $[n]$ such that agent j is a neighbor of agent i. If agent j has been infected by only one virus, say virus 1, and agent i is infected by the other virus, virus 2, then, irrespective of whether (or not) it is infected by virus 1, agent i can infect agent j with virus 2 at a rate $\epsilon^{(1)}\beta_{ji}^{(2)}$. See Fig. 1 for a depiction of the model. It is worth noting that there is no transition link from state $I^{(1,2)}$ (infected by both viruses) to state S (healthy state), as the probability that the two viruses are cured at the same time is zero. We call $\epsilon^{(m)}$ the *coupling parameter* between the viruses, and assume that each $\epsilon^{(m)}$ takes a nonnegative value. If $\epsilon^{(m)} \in (0, 1)$, it means that if a node is infected with virus m, then it is less susceptible to the other virus. If $\epsilon^{(m)} > 1$, it means that if a node is infected with virus m, it is more likely to become infected with the other virus. If $\epsilon^{(m)} = 1$ for all m, then the two viruses are independent. If $\epsilon^{(m)} = 0$ for all m, then the two viruses are competitive. We will discuss these last two special cases in-depth in Remark 1.

Let $B^{(m)} = [\beta_{ij}^{(m)}]$ for $m \in [2]$. The spread of the two viruses across the population can be represented by a two-layer graph, where the vertices of the graph correspond to the population nodes. Each layer contains a set of directed edges, $E^{(m)}$, specific to virus m, where $m = 1, 2$; there exists a directed edge from agent j to agent i in $E^{(m)}$ if, assuming agent j is infected with virus m, it can directly infect agent i. Note that there is a one-to-one correspondence between the notations $E^{(m)}$ and $B^{(m)}$ for $m \in [2]$. That is, $(i, j) \in E^{(m)}$ if, and only if, $[B^{(m)}]_{ji} \neq 0$. It is worth emphasizing that the two viruses may spread along different routes, that is, the layers corresponding to $B^{(1)}$ and $B^{(2)}$ are not necessarily the same. We call the layers corresponding to $B^{(1)}$ and $B^{(2)}$ as the spreading graphs of viruses 1 and 2, respectively.

For completeness, we provide here a full description of the 4^n-state Markov process. Each state, $Y_k(t)$, corresponds to a string s of length n, where $s_i = S$, $s_i = I^{(1)}$, $s_i = I^{(2)}$, or $s_i = I^{(1,2)}$ indicate that the ith agent is either susceptible, or infected with virus 1, or infected with virus 2, or infected with both viruses 1 and 2, respectively. The generator matrix (Norris, 1998), Q, is defined by

$$q_{kl} = \begin{cases} \delta_i^{(1)}, & \text{if } s_i = I^{(1)}, k = l + 4^{i-1} \\ \delta_i^{(2)}, & \text{if } s_i = I^{(2)}, k = l + 2(4^{i-1}) \\ \delta_i^{(1)}, & \text{if } s_i = I^{(1,2)}, k = l + 4^{i-1} \\ \delta_i^{(2)}, & \text{if } s_i = I^{(1,2)}, k = l + 2(4^{i-1}) \\ \sum_{j=1}^{n} \beta_{ij}^{(1)}(1_{s_j=I^{(1)}} + 1_{s_j=I^{(1,2)}}), & \text{if } s_i = S, k = l - 4^{i-1} \\ \sum_{j=1}^{n} \beta_{ij}^{(2)}(1_{s_j=I^{(2)}} + 1_{s_j=I^{(1,2)}}), & \text{if } s_i = S, k = l - 2(4^{i-1}) \\ \epsilon^{(2)} \sum_{j=1}^{n} \beta_{ij}^{(1)}(1_{s_j=I^{(1)}} + 1_{s_j=I^{(1,2)}}), & \text{if } s_i = I^{(2)}, k = l - 4^{i-1} \\ \epsilon^{(1)} \sum_{j=1}^{n} \beta_{ij}^{(2)}(1_{s_j=I^{(2)}} + 1_{s_j=I^{(1,2)}}), & \text{if } s_i = I^{(1)}, k = l - 2(4^{i-1}) \\ -\sum_{j \neq l} q_{jl}, & \text{if } k = l \\ 0, & \text{otherwise,} \end{cases} \tag{1}$$

for $i \in [n]$. Here virus 1 and virus 2 are propagating over a network whose infection rates are given by $\beta_{ij}^{(1)}$ and $\beta_{ij}^{(2)}$, respectively (nonnegative with $\beta_{ii}^{(1)} = \beta_{ii}^{(2)} = 0$, $\forall j$), $\delta_i^{(1)}$ and $\delta_i^{(2)}$ are the respective healing rates of the ith agent, and, again, $s_i = S$, $s_i = I^{(1)}$, $s_i = I^{(2)}$, or $s_i = I^{(1,2)}$ indicate that the ith agent is either susceptible, or infected with virus 1, or infected with virus 2, or infected with both viruses 1 and 2, respectively. The state vector $y(t)$ is defined as

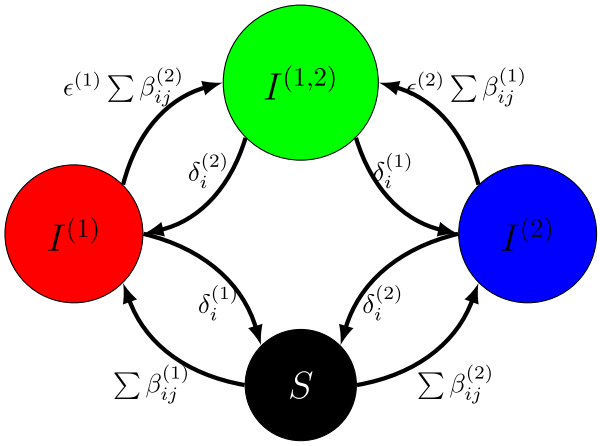

Fig. 1. The possible states and transitions for node i. State S stands for being healthy but susceptible. States $I^{(1)}$, $I^{(2)}$, and $I^{(1,2)}$ stand for being infected by virus 1, virus 2, and both virus 1 and virus 2, respectively.

$$y_k(t) = Pr[Y_k(t) = k], \tag{2}$$

with $\sum_{k=1}^{4^n} y_k(t) = 1$. The Markov process evolves as

$$\frac{dy^\top(t)}{dt} = y^\top(t)Q. \tag{3}$$

Let $v_i^{(1)}(t) = \Pr[X_i(t) = I^{(1)}]$, $v_i^{(2)}(t) = \Pr[X_i(t) = I^{(2)}]$, and $v_i^{(1,2)}(t) = \Pr[X_i(t) = I^{(1,2)}]$, where $X_i(t)$ is the random variable representing whether the ith agent is susceptible or infected with virus 1, or 2, or both. Then, for $i = \{(1), (2), (1, 2)\}$

$$(v^i)^\top(t) = y^\top(t)M^i, \tag{4}$$

where the ith columns of $M^{(1)}$, $M^{(2)}$, $M^{(1,2)}$ indicate the states in the Markov process where agent i is infected with virus 1, virus 2, and both (all the strings where $s_i = I^{(1)}$, $s_i = I^{(2)}$, and $s_i = I^{(1,2)}$), respectively, that is, $M^i = 1_{M=i}$ for $i \in \{(1), (2), (1, 2)\}$, where $M \in \mathbb{R}^{4^n \times n}$ has rows of lexicographically-ordered ternary numbers, bit reversed[3]. Therefore, $v_i^{(1)}(t)$, $v_i^{(2)}(t)$, and $v_i^{(1,2)}(t)$ reflect the summation of all probabilities where $s_i = I^{(1)}$, $s_i = I^{(2)}$, and $s_i = I^{(1,2)}$. Note that the first state of the process, which corresponds to $s_i = S$, the healthy state, for $\delta_i^{(1)}, \delta_i^{(2)} > 0$ $\forall i$, is the absorbing or sink state of the process. That is, once in the healthy state, the Markov process will never escape it. Moreover, since the healthy state is the only absorbing state, the system will converge to it with probability one (Norris, 1998).

We derive the model in (5)–(7) using a mean-field type approximation by considering the probability that node i is healthy ($X_i = S$) or infected with virus 1 ($X_i = I^{(1)}$), or virus 2 ($X_i = I^{(2)}$), or both ($X_i = I^{(1,2)}$) at time $t + \Delta t$. From (1), we have

$$\begin{aligned} &\Pr(X_i(t + \Delta t) = S | X_i(t) = I^{(1)}, X(t)) = \delta^{(1)}\Delta t + o(\Delta t) \\ &\Pr(X_i(t + \Delta t) = I^{(1)} | X_i(t) = S, X(t)) = o(\Delta t) \\ &\qquad + \textstyle\sum_{j=1}^{n} \beta_{ij}^{(1)}(1_{X_j=I^{(1)}} + 1_{X_j=I^{(1,2)}})\Delta t \\ &\Pr(X_i(t + \Delta t) = S | X_i(t) = I^{(2)}, X(t)) = \delta^{(2)}\Delta t + o(\Delta t) \\ &\Pr(X_i(t + \Delta t) = I^{(2)} | X_i(t) = S, X(t)) = o(\Delta t) \end{aligned}$$

[3] Matlab code: $M = fliplr(dec2base(0 : (4^n) - 1, 4) -' 0')$

$$+ \sum_{j=1}^{n} \beta_{ij}^{(2)}(1_{X_j=I^{(2)}} + 1_{X_j=I^{(1,2)}})\Delta t$$
$$\Pr(X_i(t+\Delta t) = I^{(1)} | X_i(t) = I^{(1,2)}, X(t)) = \delta^{(2)}\Delta t + o(\Delta t)$$
$$\Pr(X_i(t+\Delta t) = I^{(2)} | X_i(t) = I^{(1,2)}, X(t)) = \delta^{(1)}\Delta t + o(\Delta t)$$
$$\Pr(X_i(t+\Delta t) = I^{(1,2)} | X_i(t) = I^{(1)}, X(t)) = o(\Delta t) + \epsilon^{(1)} \sum_{j=1}^{n} \beta_{ij}^{(2)}(1_{X_j=I^{(2)}} + 1_{X_j=I^{(1,2)}})\Delta t$$
$$\Pr(X_i(t+\Delta t) = I^{(1,2)} | X_i(t) = I^{(2)}, X(t)) = o(\Delta t) + \epsilon^{(2)} \sum_{j=1}^{n} \beta_{ij}^{(2)}(1_{X_j=I^{(1)}} + 1_{X_j=I^{(1,2)}})\Delta t$$
$$\vdots$$

Letting Δt go to zero and taking expectations of $1_{X_i(t)=I^{(1)}}$, $1_{X_i(t)=I^{(2)}}$, and $1_{X_i(t)=I^{(1,2)}}$ gives

$$\frac{d\,\mathrm{E}(1_{X_i(t)=I^{(1)}})}{dt} = -\delta^{(1)}\,\mathrm{E}(1_{X_i(t)=I^{(1)}}) + \delta^{(2)}\,\mathrm{E}(1_{X_i(t)=I^{(1,2)}}) + \mathrm{E}\left(1_{X_i(t)=S}\sum_{j=1}^{n}\beta_{ij}^{(1)}(1_{X_j(t)=I^{(1)}} + 1_{X_j(t)=I^{(1,2)}})\right) - \mathrm{E}\left(1_{X_i(t)=I^{(1)}}\epsilon^{(1)}\sum_{j=1}^{n}\beta_{ij}^{(2)}(1_{X_j(t)=I^{(2)}} + 1_{X_j(t)=I^{(1,2)}})\right),$$
$$\frac{d\,\mathrm{E}(1_{X_i(t)=I^{(2)}})}{dt} = -\delta^{(2)}\,\mathrm{E}(1_{X_i(t)=I^{(2)}}) + \delta^{(1)}E(1_{X_i(t)=I^{(1,2)}}) + \mathrm{E}\left(1_{X_i(t)=S}\sum_{j=1}^{n}\beta_{ij}^{(2)}(1_{X_j(t)=I^{(2)}} + 1_{X_j(t)=I^{(1,2)}})\right) - \mathrm{E}\left(1_{X_i(t)=I^{(2)}}\epsilon^{(2)}\sum_{j=1}^{n}\beta_{ij}^{(1)}(1_{X_j(t)=I^{(1)}} + 1_{X_j(t)=I^{(1,2)}})\right),$$
$$\frac{d\,\mathrm{E}(1_{X_i(t)=I^{(1,2)}})}{dt} = -(\delta^{(1)} + \delta^{(2)})\,\mathrm{E}(1_{X_i(t)=I^{(1,2)}}) + \mathrm{E}\left(1_{X_i(t)=I^{(1)}}\epsilon^{(1)}\sum_{j=1}^{n}\beta_{ij}^{(2)}(1_{X_j(t)=I^{(2)}} + 1_{X_j(t)=I^{(1,2)}})\right) + \mathrm{E}\left(1_{X_i(t)=I^{(2)}}\epsilon^{(2)}\sum_{j=1}^{n}\beta_{ij}^{(1)}(1_{X_j(t)=I^{(1)}} + 1_{X_j(t)=I^{(1,2)}})\right).$$

Using the above equations, $\Pr(z) = E(1_z)$, $x_i^{(1)}(t) = \Pr(X_i(t) = I^{(1)})$, $x_i^{(2)}(t) = \Pr(X_i(t) = I^{(2)})$, $z_i(t) = \Pr(X_i(t) = I^{(1,2)})$, $(1 - x_i^{(1)}(t) - x_i^{(2)}(t) - z_i(t)) = \Pr(X_i(t) = S)$, and approximating $\Pr(X_i(t) = I^{(1)}, X_j(t) = I^{(1)}) \approx x_i^{(1)}(t)x_j^{(1)}(t)$, $\Pr(X_i(t) = I^{(1)}, X_j(t) = I^{(2)}) \approx x_i^{(1)}(t)x_j^{(2)}(t)$, $\Pr(X_i(t) = I^{(1)}, X_j(t) = I^{(1,2)}) \approx x_i^{(1)}(t)z_j(t)$, $\Pr(X_i(t) = I^{(2)}, X_j(t) = I^{(2)}) \approx x_i^{(2)}(t)x_j^{(2)}(t)$, $\Pr(X_i(t) = I^{(2)}, X_j(t) = I^{(1,2)}) \approx x_i^{(2)}(t)z_j(t)$ (which inaccurately assumes independence, as is done in the single-virus (Van Mieghem et al., 2009) and bi-virus cases (Liu et al., 2019)) gives

$$\dot{x}_i^{(1)}(t) = -\delta_i^{(1)}x_i^1(t) + \delta_i^{(2)}z_i(t) + (1 - x_i^{(1)}(t) - x_i^{(2)}(t) - z_i(t))\sum_{j=1}^{n}\beta_{ij}^{(1)}(x_j^{(1)}(t) + z_j(t)) - x_i^{(1)}(t)\epsilon^{(1)}\sum_{j=1}^{n}\beta_{ij}^{(2)}(x_j^{(2)}(t) + z_j(t)), \tag{5}$$
$$\dot{x}_i^{(2)}(t) = -\delta_i^{(2)}x_i^{(2)}(t) + \delta_i^{(1)}z_i(t) + (1 - x_i^{(1)}(t) - x_i^{(2)}(t) - z_i(t))\sum_{j=1}^{n}\beta_{ij}^{(2)}(x_j^{(2)}(t) + z_j(t)) - x_i^{(2)}(t)\epsilon^{(2)}\sum_{j=1}^{n}\beta_{ij}^{(1)}(x_j^{(1)}(t) + z_j(t)), \tag{6}$$
$$\dot{z}_i(t) = -(\delta_i^{(1)} + \delta_i^{(2)})z_i(t) + x_i^{(1)}(t)\epsilon^{(1)}\sum_{j=1}^{n}\beta_{ij}^{(2)}(x_j^{(2)}(t) + z_j(t)) + x_i^{(2)}(t)\epsilon^{(2)}\sum_{j=1}^{n}\beta_{ij}^{(1)}(x_j^{(1)}(t) + z_j(t)). \tag{7}$$

The above equations can be combined into vector form, as follows:

$$\dot{x}^{(1)}(t) = -D^{(1)}x^{(1)}(t) + D^{(2)}z(t) + (I - X^{(1)}(t) - X^{(2)}(t) - Z(t))B^{(1)}(x^{(1)}(t) + z(t)) - \epsilon^{(1)}X^{(1)}(t)B^{(2)}(x^{(2)}(t) + z(t)), \tag{8}$$
$$\dot{x}^{(2)}(t) = -D^{(2)}x^{(2)}(t) + D^{(1)}z(t) + (I - X^{(1)}(t) - X^{(2)}(t) - Z(t))B^{(2)}(x^{(2)}(t) + z(t)) - \epsilon^{(2)}X^{(2)}(t)B^{(2)}(x^{(1)}(t) + z(t)), \tag{9}$$
$$\dot{z}(t) = -(D^{(1)} + D^{(2)})z(t) + \epsilon^{(1)}X^{(1)}(t)B^{(2)}(x^{(2)}(t) + z(t)) + \epsilon^{(2)}X^{(2)}(t)B^{(1)}(x^{(1)}(t) + z(t)), \tag{10}$$

where $x^{(1)}(t)$, $x^{(2)}(t)$, $z(t)$ are the column vectors obtained by stacking $x_i^{(1)}(t)$, $x_i^{(2)}(t)$, and $z_i(t)$, respectively, $B^{(1)}$, $B^{(2)}$ are the matrices of $\beta_{ij}^{(1)}$, $\beta_{ij}^{(2)}$, respectively, $X^{(1)}(t) = \mathrm{diag}(x^{(1)}(t))$, $X^{(2)}(t) = \mathrm{diag}(x^{(2)}t)$, $Z(t) = \mathrm{diag}(z(t))$, $D^{(1)} = \mathrm{diag}(\delta^{(1)})$, and $D^{(2)} = \mathrm{diag}(\delta^{(2)})$. For completeness, to illustrate the effectiveness of the first-order approximation, we compare (1)–(4) and (8)–(10) via simulations in Section 8.1.

Note that an agent i could be interpreted as either an individual i or a subpopulation i. The two interpretations are equivalent, since the group model that we employ in this paper can also be derived from a group model interpretation of the original stochastic model; see (Paré, Liu, Beck, Kirwan, & Başar, 2020). In particular, the former models the probability of each individual being infected over time, while the latter models the fraction of a subpopulation being infected. Thus, there are no abrupt transitions from a susceptible state to one of the infected states for an entire subpopulation. The states of each subpopulation are continuously changing variable values between 0 and 1. Further, it is assumed that each subpopulation is well mixed/connected, which is the same assumption as in classical single-population epidemic models (Kermack & McKendrick, 1927).

Remark 1. We consider two special cases of the model. First, let $\epsilon^{(1)} = \epsilon^{(2)} = 0$, and $\delta_i^{(1)} + \delta_i^{(2)} > 0$ for all $i \in [n]$. Then, the system defined by (8)–(10) simplifies to

$$\dot{x}^{(1)}(t) = -D^{(1)}x^{(1)}(t) + D^{(2)}z(t) + (I - X^{(1)}(t) - X^{(2)}(t) - Z(t))B^{(1)}(x^{(1)}(t) + z(t)), \tag{11}$$
$$\dot{x}^{(2)}(t) = -D^{(2)}x^{(2)}(t) + D^{(1)}z(t) + (I - X^{(1)}(t) - X^{(2)}(t) - Z(t))B^{(2)}(x^{(2)}(t) + z(t)), \tag{12}$$
$$\dot{z}(t) = -(D^{(1)} + D^{(2)})z(t). \tag{13}$$

In this case, since the matrix $D^{(1)} + D^{(2)}$ is positive definite, it follows that $z(t)$ converges to $\mathbf{0}$ exponentially fast, and thus the system will eventually become a competitive bi-virus model which has been studied in (Liu et al., 2016, 2019; Prakash, Beutel, Rosenfeld, & Faloutsos, 2012; Santos, Moura, & Xavier, 2015).

In the second case, we let $\epsilon^{(1)} = \epsilon^{(2)} = 1$. To proceed, we define $y_i^{(1)}(t) = x_i^{(1)}(t) + z_i(t)$ and $y_i^{(2)}(t) = x_i^{(2)}(t) + z_i(t)$ for each $i \in [n]$, which represents the total probabilities of agent i being infected by viruses 1 and 2, respectively. From (5)–(7), the dynamics of $y_i^{(1)}$ and $y_i^{(2)}$ are

$$\dot{y}_i^{(1)}(t) = -\delta_i^{(1)}y_i^{(1)}(t) + (1 - y_i^{(1)}(t))\sum_{j=1}^{n}\beta_{ij}^{(1)}y_j^{(1)}(t),$$
$$\dot{y}_i^{(2)}(t) = -\delta_i^{(2)}y_i^{(2)}(t) + (1 - y_i^{(2)}(t))\sum_{j=1}^{n}\beta_{ij}^{(2)}y_j^{(2)}(t),$$

which are two independent single SIS dynamics. Therefore, the system defined by (8)–(10) subsumes both the single SIS virus (two single, independent viruses) and the competitive SIS virus models.

3. Problem formulation

In this section, we formally state the problems of interest, and the key assumptions needed for ensuring that the model introduced in Section 2 is well defined.

3.1. Problem statements

With respect to the model in (8)–(10), we consider the following questions:

(i) Can a sufficient condition be identified under which, irrespective of the initial state, the dynamics converge asymptotically to the healthy state?
(ii) Can a sufficient condition be identified for virus m, such that for any $x^{(m)}(0) \neq \mathbf{0}$ the dynamics asymptotically converge to the single-virus endemic equilibrium of virus m, for $m = 1, 2$?
(iii) Can a sufficient condition be identified for local exponential convergence to the boundary equilibrium of virus m, for $m = 1, 2$?
(iv) Can a necessary condition(s) be provided for local exponential convergence to the boundary equilibrium of virus m, for $m = 1, 2$?
(v) Is it possible for equilibria of the kind (a) $(\hat{x}^{(1)}, \hat{x}^{(2)}, \mathbf{0})$ with $\hat{x}^{(1)}, \hat{x}^{(2)} > \mathbf{0}$, and (b) $(\mathbf{0}, \mathbf{0}, \hat{z})$ with $\hat{z} > \mathbf{0}$, to exist?
(vi) Can a necessary condition be identified for the existence of the coexisting equilibria (a) $(\hat{x}^{(1)}, \mathbf{0}, \hat{z})$, with $\hat{x}^{(1)}, \hat{z} > \mathbf{0}$, or (b) $(\mathbf{0}, \hat{x}^{(2)}, \hat{z})$, with $\hat{x}^{(2)}, \hat{z} > \mathbf{0}$?
(vii) Can a condition be identified that rules out an arbitrary point $(\hat{x}^{(1)}, \hat{x}^{(2)}, \hat{z})$ with $\hat{x}^{(1)}, \hat{x}^{(2)}, \hat{z} > \mathbf{0}$ as a coexisting equilibrium?
(viii) Is the system monotone?

3.2. Key assumptions and preliminaries

We make the following assumptions on the model to ensure that it is well defined.

Assumption 1. For all $i \in [n]$, we have $x_i^{(1)}(0), x_i^{(2)}(0), z_i(0), (1 - x_i^{(1)}(0) - x_i^{(2)}(0) - z_i(0)) \in [0, 1]$.

Assumption 2. For all $i \in [n]$, we have $\delta_i^{(1)}, \delta_i^{(2)} \geq 0$. The matrices $B^{(1)}$ and $B^{(2)}$ are nonnegative and irreducible.

Assumption 1 guarantees that the initial infection level with respect to each virus m ($m \in [2]$) in each node $i \in [n]$ lies in the set $[0, 1]$, whereas Assumption 2 ensures that the healing and infection rates are nonnegative, and that the spreading graphs for virus 1 and 2 are strongly connected.

Define the set

$$\mathcal{D} := \{(x^{(1)}, x^{(2)}, z) \mid x^{(1)} \geq \mathbf{0},\ x^{(2)} \geq \mathbf{0},\ z \geq \mathbf{0},\ x^{(1)} + x^{(2)} + z \leq \mathbf{1}\} \tag{14}$$

The following lemma establishes that the set $\mathcal{D}$ is positively invariant with respect to the system (8)–(10).

Lemma 1. *Under Assumptions 1 and 2, $x_i^{(1)}(t), x_i^{(2)}(t), z(t), x_i^{(2)}(t) + x_i^{(2)}(t) + z(t) \in [0, 1]$ for all $i \in [n]$ and $t \geq 0$.*

Proof. See the proof of (Gracy et al., 2024, Lemma 1). ■

Lemma 1 implies that the set $\mathcal{D}$ is positively invariant with respect to the system defined by (8)–(10). Since $x_i^{(1)}$, $x_i^{(2)}$, and z_i denote the probabilities of sickness of agent i, or fractions of group i, infected by viruses 1, 2, and both 1 and 2 simultaneously, respectively, and $1 - x_i^{(1)} - x_i^{(2)} - z_i$ denotes the probability of agent i, or fraction of group i that is healthy, it is natural to assume that their initial values are in the interval $[0, 1]$, since otherwise the values will be devoid of any physical meaning for the spread model considered here.

Let $(\hat{x}^{(1)}, \hat{x}^{(2)}, \hat{z})$ be an equilibrium of system (8)–(10). Then, the Jacobian matrix of the equilibrium, denoted by $J(\hat{x}^{(1)}, \hat{x}^{(2)}, \hat{z})$, with $\hat{B}^{(i)} = \operatorname{diag}(B^{(i)}(\hat{x}^{(i)} + \hat{z}))$, $\hat{Z}^{(i)} = Z\operatorname{diag}(B^{(i)}\mathbf{1})$, $i \in [2]$, and $W = (I - \hat{X}^{(1)} - \hat{X}^{(2)} - \hat{Z})$, is as given in (15) (see Box I), where

$$J_{1,1} = WB^{(1)} - D^{(1)} - \hat{B}^{(1)} - \epsilon^{(1)}\hat{B}^{(2)} \tag{16}$$

$$J_{2,2} = WB^{(2)} - D^{(2)} - \hat{B}^{(2)} - \epsilon^{(2)}\hat{B}^{(1)} \tag{17}$$

$$J_{3,3} = -D^{(1)} - D^{(2)} + \epsilon^{(1)}\hat{X}^{(1)}B^{(2)} + \epsilon^{(2)}\hat{X}^{(2)}B^{(1)}. \tag{18}$$

4. Analysis of the disease-free equilibrium

In this section, we analyze the system defined by (8)–(10). It is easy to see that $(\mathbf{0}, \mathbf{0}, \mathbf{0})$ is an equilibrium of the system defined by (8)–(10). We call it the DFE, or the healthy state. We focus on identifying conditions under which the healthy state is stable. The following proposition provides a necessary and sufficient condition for local exponential convergence to the healthy state.

Proposition 1. *Consider system (8)–(10) under Assumptions 1 and 2. The healthy state is locally exponentially stable if, and only if, $s(-D^{(1)} + B^{(1)}) < 0$, $s(-D^{(2)} + B^{(2)}) < 0$, and $\delta_i^{(1)} + \delta_i^{(2)} > 0$ for all $i \in [n]$. If $s(-D^{(1)} + B^{(1)}) > 0$ or if $s(-D^{(2)} + B^{(2)}) > 0$, then the healthy state is unstable.*

Proof. From (15), we have

$$J(\mathbf{0}, \mathbf{0}, \mathbf{0}) = \begin{bmatrix} B^{(1)} - D^{(1)} & 0 & B^{(1)} + D^{(2)} \\ 0 & B^{(2)} - D^{(2)} & WB^{(2)} + D^{(1)} \\ 0 & 0 & -D^{(1)} - D^{(2)} \end{bmatrix}. \tag{19}$$

Thus, from (Khalil, 2002, Theorem 4.15 and Corollary 4.3), the healthy state is locally exponentially stable if, and only if, $s(-D^{(1)} + B^{(1)}) < 0$, $s(-D^{(2)} + B^{(2)}) < 0$, and $\delta_i^{(1)} + \delta_i^{(2)} > 0$ for all $i \in [n]$. Note that if $s(-D^{(1)} + B^{(1)}) > 0$ or if $s(-D^{(2)} + B^{(2)}) > 0$, then $s(J(\mathbf{0}, \mathbf{0}, \mathbf{0})) > 0$. The claim on instability then follows from (Khalil, 2002, Theorem 4.7). ■

Note that, on the one hand, the guarantees provided by Proposition 1 are limited in the sense that they concern trajectories that originate in a small neighborhood of the healthy state. On the other hand, no restrictions, besides nonnegativity, are imposed on $\epsilon^{(m)}$, $m = 1, 2$. Simulations, as we see in Section 8.2, indicate that the region of attraction for the healthy state depends on the choices of $\epsilon^{(m)}$, $m = 1, 2$. In particular, if the initial state of system (8)–(10) is very close to the healthy state, then, even for a larger value of $\epsilon^{(m)}$, $m = 1, 2$, the dynamics converge to the healthy state. If the initial state of system (8)–(10) is not too close to the healthy state, then for large values of $\epsilon^{(m)}$, the dynamics do not converge to the healthy state; see Fig. 9 in Section 8.2.

The following theorem guarantees global convergence to the healthy state, but with the following caveats: (i) the speed of convergence is slower, and (ii) more restrictions on $\epsilon^{(m)}$, $m = 1, 2$, have to be imposed.

Theorem 1. *Under Assumptions 1 and 2, if $\epsilon^{(1)}, \epsilon^{(2)} \in [0, 1]$, $s(B^{(1)} - D^{(1)}) \leq 0$ and $s(B^{(2)} - D^{(2)}) \leq 0$, then the healthy state is the unique equilibrium of (8)–(10), and the system defined by (8)–(10) asymptotically converges to the healthy state for any initial state in $\mathcal{D}$, as defined in (14).*

Proof. See the Appendix. ■

Theorem 1 answers Question (i) raised in Section 3.1.

5. Persistence of viruses

We call an equilibrium $(\hat{x}^{(1)}, \hat{x}^{(2)}, \hat{z})$ an endemic equilibrium if it is not the healthy state, $(\mathbf{0}, \mathbf{0}, \mathbf{0})$. It turns out that if either (or both) of the spectral abscissa conditions in Theorem 1 are violated, then at least one of the viruses pervades the population. We detail the same in the rest of this section.

$$J(\hat{x}^{(1)}, \hat{x}^{(2)}, \hat{z}) = \tag{15}$$
$$\begin{bmatrix} J_{1,1} & -\hat{B}^{(1)} - \epsilon^{(1)}\hat{X}^{(1)}B^{(2)} & WB^{(1)} + D^{(2)} - \hat{B}^{(1)} - \epsilon^{(1)}\hat{X}^{(1)}B^{(2)} \\ -\hat{B}^{(2)} - \epsilon^{(2)}\hat{X}^{(2)}B^{(1)} & J_{2,2} & WB^{(2)} + D^{(1)} - \hat{B}^{(2)} - \epsilon^{(2)}\hat{X}^{(2)}B^{(1)} \\ \epsilon^{(1)}\hat{B}^{(2)} + \epsilon^{(2)}\hat{X}^{(2)}B^{(1)} & \epsilon^{(2)}\hat{B}^{(1)} + \epsilon^{(1)}\hat{X}^{(1)}B^{(2)} & J_{3,3} \end{bmatrix}.$$

Box I.

5.1. Existence, uniqueness and stability of the single virus endemic equilibria

We consider the scenario in which either $s(B^{(1)} - D^{(1)})$ or $s(B^{(2)} - D^{(2)})$ is greater than zero. Without loss of generality, we assume that $s(B^{(1)} - D^{(1)}) > 0$, $\epsilon^{(1)} \in [0, 1]$, and $s(B^{(2)} - D^{(2)}) \leq 0$. We denote by $\hat{x}^{(1)}$ (resp. $\hat{x}^{(2)}$) the single-virus endemic equilibrium corresponding to virus 1 (resp. virus 2). We have the following result.

Theorem 2. *Under Assumptions 1 and 2, if $s(B^{(1)} - D^{(1)}) > 0$, $\epsilon^{(1)} \in [0, 1]$, and $s(B^{(2)} - D^{(2)}) \leq 0$, then system (8)–(10) has a unique endemic equilibrium $(\hat{x}^{(1)}, \mathbf{0}, \mathbf{0})$ with $\hat{x}^{(1)} \gg \mathbf{0}$, and the system asymptotically converges to the endemic equilibrium for any initial state in $\mathcal{D} \setminus \{(\mathbf{0}, x^{(2)}, \mathbf{0}) | \mathbf{0} \leq x^{(2)} \leq \mathbf{1}\}$, where $\mathcal{D}$ is as defined in (14).*

Proof. See the Appendix. □

Theorem 2 establishes the existence, uniqueness, and asymptotic stability of the single-virus endemic equilibrium corresponding to virus 1. An analogous result holds for virus 2; the details are omitted in the interest of space. Theorem 2 answers Question (ii) raised in Section 3.1. Note that, for a single virus system, assuming that the existence of the endemic equilibrium is guaranteed, an exact characterization of the same has been provided in (Mei et al., 2017, Theorem 4.3, statement (iii)(b)).

Combining Theorems 1 and 2, we obtain a necessary and sufficient condition for the healthy state to be the unique equilibrium of the coupled bi-virus system, as stated below.

Corollary 1. *Consider system (8)–(10) under Assumptions 1 and 2. Suppose further that $\epsilon^{(1)}, \epsilon^{(2)} \in [0, 1]$. The healthy state is the unique equilibrium if, and only if, each of the following conditions are satisfied (i) $s(B^{(1)} - D^{(1)}) \leq 0$ and (ii) $s(B^{(2)} - D^{(2)}) \leq 0$.*

5.2. Both viruses pervading the system

Note that Theorem 2 accounts for the case where exactly one of the viruses pervades the system, or, in other words, exactly one of the spectral abscissa conditions in Theorem 1 is violated. However, what happens when *both* the spectral abscissa conditions in Theorem 1 are violated? The following corollary answers this question.

Corollary 2. *Consider system (8)–(10) under Assumptions 1 and 2. Suppose further that $\epsilon^{(1)} = \epsilon^{(2)} = \epsilon \in [0, 1]$. If $s(B^{(1)} - D^{(1)}) > 0$ and $s(B^{(2)} - D^{(2)}) > 0$, then system (8)–(10) has at least three equilibria, namely, the healthy state $(\mathbf{0}, \mathbf{0}, \mathbf{0})$, which is unstable; the single virus endemic equilibrium corresponding to virus 1 $(\hat{x}^{(1)}, \mathbf{0}, \mathbf{0})$; and the single virus endemic equilibrium corresponding to virus 2 $(\mathbf{0}, \hat{x}^{(2)}, \mathbf{0})$.*

Proof. See the Appendix. ■

The equilibria of the kind $(\hat{x}^{(1)}, \mathbf{0}, \mathbf{0})$ and $(\mathbf{0}, \hat{x}^{(2)}, \mathbf{0})$ are hereafter referred to as the *boundary* equilibria. Note that $\hat{x}^{(1)}$ and $\hat{x}^{(2)}$ are asymptotically stable in the single virus (i.e., one of the two viruses has died out) systems corresponding to virus 1 and virus 2, respectively; when both viruses pervade the network, the stability of $(\hat{x}^{(1)}, \mathbf{0}, \mathbf{0})$ and $(\mathbf{0}, \hat{x}^{(2)}, \mathbf{0})$, in even the local (let alone global) sense, is not guaranteed. As such, in the rest of this section we will focus on identifying a sufficient condition (resp. some necessary conditions) for local exponential stability of the boundary equilibria.

We need the following assumption, which is slightly stronger than Assumption 2.

Assumption 3. For all $i \in [n]$, we have $\delta_i^{(1)}, \delta_i^{(2)} > 0$. The matrices $B^{(1)}$ and $B^{(2)}$ are nonnegative and irreducible.

The following theorem provides a sufficient condition for local exponential stability of the boundary equilibrium $(\hat{x}^{(1)}, \mathbf{0}, \mathbf{0})$.

Theorem 3. *Consider system (8)–(10) under Assumption 1 and 3. Suppose that (i) $\epsilon^{(1)} = \epsilon^{(2)} = \epsilon \in [0, 1]$, (ii) $s(-D^{(1)} + B^{(1)}) > 0$, and (iii) $s(-D^{(2)} + B^{(2)}) > 0$. The equilibrium point $(\hat{x}^{(1)}, \mathbf{0}, \mathbf{0})$ is locally exponentially stable if*

(i) $s(-D^{(2)} + (I - \hat{X}^{(1)})B^{(2)}) < 0$; *and*

(ii) $s\Big((-D^{(1)} - D^{(2)} + \epsilon\hat{X}^{(1)}B^{(2)}) - (\epsilon\hat{B}^{(1)} + \epsilon\hat{X}^{(1)}B^{(2)})(-D^{(2)} + (I - \hat{X}^{(1)})B^{(2)} - \epsilon\hat{B}^{(1)})^{-1}((I - \hat{X}^{(1)})B^{(2)} + D^{(1)})\Big) < 0.$

Proof. See the Appendix. ■

Theorem 3 answers Question (iii) raised in Section 3.1.

The following proposition provides necessary conditions for local exponential stability of the equilibrium $(\hat{x}^{(1)}, \mathbf{0}, \mathbf{0})$.

Proposition 2. *Consider system (8)–(10) under Assumption 1 and 3. Suppose that $\epsilon^{(1)} = \epsilon^{(2)} = \epsilon \in [0, 1]$, and that $s(-D^{(1)} + B^{(1)}) > 0$. The equilibrium point $(\hat{x}^{(1)}, \mathbf{0}, \mathbf{0})$ is locally exponentially stable only if each of the following conditions are satisfied*

(i) $s(-D^{(2)} + (I - \hat{X}^{(1)})B^{(2)} - \epsilon\hat{B}^{(1)}) < 0$; *and*

(ii) $s\Big((-D^{(1)} - D^{(2)} + \epsilon\hat{X}^{(1)}B^{(2)}) - (\epsilon\hat{B}^{(1)} + \epsilon\hat{X}^{(1)}B^{(2)})(-D^{(2)} + (I - \hat{X}^{(1)})B^{(2)} - \epsilon\hat{B}^{(1)})^{-1}((I - \hat{X}^{(1)})B^{(2)} + D^{(1)})\Big) < 0.$

Proof. See the Appendix. ■

Proposition 2 answers (iv) raised in Section 3.1.

Remark 2. Note that, in general, there is a gap between the sufficient condition in Theorem 3 and the necessary conditions in Proposition 2. However, if $\epsilon^{(m)} = 0$ for $m = 1, 2$, the sufficient condition in Theorem 3 and the necessary conditions in Proposition 2 coincide to yield a necessary and sufficient condition for local exponential convergence to $(\hat{x}^{(1)}, \mathbf{0}, \mathbf{0})$. Further, by Assumption 3, $\delta_i^{(1)} > 0$ and $\delta_i^{(2)} > 0$ for each $i \in [n]$. Hence, if

$\epsilon^{(m)} = 0$ for $m = 1, 2$, then condition (ii) in both Theorem 3 and Proposition 2 is always satisfied. As a consequence, condition (i) in Theorem 3 becomes a necessary and sufficient condition, which is consistent with (Ye et al., 2022, Theorem 3.10).

Remark 3. Theorem 3 pertains to local exponential stability of the boundary equilibrium $(\hat{x}^{(1)}, \mathbf{0}, \mathbf{0})$. It is of interest to know when the boundary equilibrium $(\hat{x}^{(1)}, \mathbf{0}, \mathbf{0})$ can be globally stable. A partial answer is as follows: Suppose that the conditions in Theorem 3 are satisfied. Suppose that $\epsilon^{(1)} = \epsilon^{(2)} = 0$. Then if the system (8)–(10) has no coexistence equilibria (guaranteed by, for instance, $B^{(2)} > B^{(1)}$ (Janson, Gracy, Paré, Sandberg, & Johansson, 2020, Corollary 2)), then the boundary equilibrium $(\hat{x}^{(1)}, \mathbf{0}, \mathbf{0})$ is globally asymptotically stable; see (Ye et al., 2022, Corollary 3.16)

We next present a result for instability of the boundary equilibrium $(\hat{x}^{(1)}, \mathbf{0}, \mathbf{0})$.

Corollary 3. *Consider system (8)–(10) under Assumption 1 and 3. Suppose that $\epsilon^{(1)} = \epsilon^{(2)} = \epsilon \in [0, 1]$, and that $s(-D^{(1)} + B^{(1)}) > 0$. If $s(-D^{(1)} - D^{(2)} + \epsilon\hat{X}^{(1)}B^{(2)}) > 0$, then the equilibrium $(\hat{x}^{(1)}, \mathbf{0}, \mathbf{0})$ is unstable.*

Proof. See the Appendix. ■

Note that by suitably changing the notations of Theorem 3, Proposition 2, and Corollary 3, we can obtain a sufficient condition, necessary conditions, and a condition for instability, respectively, for the boundary equilibrium $(\mathbf{0}, \hat{x}^{(2)}, \mathbf{0})$.

6. Analysis of coexisting equilibria

Equilibria of the kind $(\hat{x}^{(1)}, \hat{x}^{(2)}, \hat{z})$ with at least any two of $\hat{x}^{(1)}, \hat{x}^{(2)}, \hat{z}$ being non-zero vectors, are referred to as *coexisting equilibria*. In this section, we show that certain kinds of coexisting equilibria cannot exist, and we focus on identifying necessary conditions for the existence of certain other kinds of coexisting equilibria.

6.1. Impossibility of existence of a certain kind of coexisting equilibria

It is well known that for the competitive bivirus case (i.e., $\epsilon^{(m)} = 0$ for $m = 1, 2$), one of the possible equilibria is the so-called coexistence equilibrium, where separate fractions of each node is infected by virus 1 and virus 2 (Janson et al., 2020; Liu et al., 2019; Ye et al., 2022). More formally, these are equilibria of the kind $(\hat{x}^{(1)}, \hat{x}^{(2)})$ with $\mathbf{0} \ll \hat{x}^{(1)} \ll \mathbf{1}$, $\mathbf{0} \ll \hat{x}^{(2)} \ll \mathbf{1}$ and $\hat{x}^{(1)} + \hat{x}^{(2)} \ll \mathbf{1}$. It is natural to wonder whether similar equilibria could exist even when $\epsilon^{(m)} > 0$ for $m = 1, 2$. It turns out, however, that such coexistence equilibria do *not* exist for coupled bivirus systems. The following proposition formalizes this.

Proposition 3. *Consider system (8)–(10) under Assumption 1 and 2. Suppose that $\epsilon^{(m)} > 0$ for some $m \in [2]$. There does not exist a coexisting equilibrium of the form $(\hat{x}^{(1)}, \hat{x}^{(2)}, \mathbf{0})$ with $\hat{x}^{(1)}, \hat{x}^{(2)} > \mathbf{0}$.*

Proof. See the Appendix. ■

In a similar vein to Proposition 3, the following proposition states that the coupled bivirus system cannot have an equilibrium where a fraction of each node is infected by both viruses at the same time, but that no fraction of any node is infected only by one of the viruses.

Proposition 4. *Consider system (8)–(10) under Assumption 3. There does not exist an equilibrium of the form $(\mathbf{0}, \mathbf{0}, \hat{z})$, where $\hat{z} > \mathbf{0}$.*

Proof. See the proof of (Gracy et al., 2024, Proposition 4) ■

Taken together, Propositions 3 and 4 answer, in the negative, Question (v) raised in Section 3.1. In so doing, Propositions 3 and 4 restrict the set of possible endemic equilibria for the coupled bivirus system.

6.2. Necessary conditions for existence of certain kinds of coexisting equilibria

While Section 6.1 has dealt with the impossibility of existence of certain kinds of coexisting equilibria, in this subsection we are interested in identifying some necessary conditions for the existence of certain other kinds of coexisting equilibria. We begin by presenting a necessary condition for the existence of a coexisting equilibrium where for each node the fraction infected only by virus 1 is non-zero, by both viruses 1 and 2 is non-zero, but only by virus 2 is zero.

Proposition 5. *Consider system (8)–(10) under Assumption 3. Suppose that (i) $\rho((D^{(1)})^{-1}B^{(1)}) > 1$, and (ii) $\epsilon^{(1)} = \epsilon^{(2)} = \epsilon$ with $\epsilon \in (0, 1)$. Then, there exists an equilibrium $(\hat{x}^{(1)}, \mathbf{0}, \hat{z})$ with $\hat{x}^{(1)}, \hat{z} > \mathbf{0}$ only if $\rho((D^{(1)})^{-1}(B^{(2)})) \geq 1$.*

Proof. See the proof of (Gracy et al., 2024, Proposition 5). ■

By following analogous arguments as in the proof of Proposition 5, it can be shown that there exists an equilibrium $(\mathbf{0}, \hat{x}^{(2)}, \hat{z})$ only if $\rho((D^{(2)})^{-1}(B^{(1)})) \geq 1$. Thus, Proposition 5 conclusively answers Question (vi) raised in Section 3.1.

Next, we present a condition that rules out a *given* point in the state space as a coexisting equilibrium where each node has (i) a fraction that is infected only by virus 1; (ii) a fraction that is infected only by virus 2; and (iii) a fraction that is infected by both viruses 1 and 2. To this end, we need the following assumption.

Assumption 4. The healing and infection rates are the same for each virus. That is, $\delta_i^{(1)} = \delta_i^{(2)}$ for all $i \in [n]$, and $\beta_{ij}^{(1)} = \beta_{ij}^{(2)}$ for all $i = j \in [n]$ and $(i, j) \in \mathcal{E}$.

In words, Assumption 4 states that two identical heterogeneous viruses spread over the same graph. This implies that $D^{(1)} = D^{(2)} = D$, and $B^{(1)} = B^{(2)} = B$. With Assumption 4 in place, we have the following result.

Proposition 6. *Consider system (8)–(10) under Assumption 1, 3 and 4. Suppose further that $\epsilon^{(1)} = \epsilon^{(2)} = \epsilon \geq 0$. Then, there exists an equilibrium $(\hat{x}^{(1)}, \hat{x}^{(2)}, \hat{z})$, where $\hat{x}^{(1)}, \hat{x}^{(2)}, \hat{z} > \mathbf{0}$, only if $\rho((I - \hat{X}^{(1)} - \hat{X}^{(2)} - \hat{Z})D^{-1}B) < 1$.*

Proof. See the proof of (Gracy et al., 2024, Proposition 6).

Proposition 6 answers Question (vii) raised in Section 3.1.

Note that Proposition 6 is, in itself, *not* a necessary condition. That is, if a given point $(\hat{x}^{(1)}, \hat{x}^{(2)}, \hat{z})$, where $\hat{x}^{(1)}, \hat{x}^{(2)}, \hat{z} > \mathbf{0}$, were to not fulfill the condition in Proposition 6, it does not mean that there cannot exist another point, say, $(\tilde{x}^{(1)}, \tilde{x}^{(2)}, \tilde{z})$, where $\tilde{x}^{(1)}, \tilde{x}^{(2)}, \tilde{z} > \mathbf{0}$, that satisfies the condition in Proposition 6. Of course, if every point in the state space violates the aforementioned condition, then no equilibrium of the form $(\hat{x}^{(1)}, \hat{x}^{(2)}, \hat{z})$, $\hat{x}^{(1)}, \hat{x}^{(2)}, \hat{z} > \mathbf{0}$, can exist.

7. Monotonicity (or lack thereof) of the coupled bivirus system

The discussion heretofore has centered around existence, uniqueness and stability of certain specific equilibria. It is natural to seek a more general perspective on the coupled bi-virus model, which is the main focus of this section.

With $\epsilon^{(1)} = \epsilon^{(2)} = 0$ (i.e., the competitive bivirus case), the system defined by (8)–(10) is monotone; see (Ye et al., 2022, Lemma 3.3). This section seeks to answer whether the same holds for the case when $\epsilon^{(1)} > 0$ and/or $\epsilon^{(2)} > 0$. To this end, first we introduce a graph structure, and then use this graph to provide a conclusive answer.

7.1. Construction of the graph associated with the Jacobian of a non-linear system

Consider a system $\dot{x} = f(x)$, and let $J(\cdot)$ denote the Jacobian of this system. It turns out that we can construct a graph associated with $J(\cdot)$; call this graph $\bar{G}$. The construction follows the outline provided in (Sontag, 2007). More specifically, the number of nodes in the graph $\bar{G}$ equals the number of rows (resp. columns) of $J(\cdot)$, whereas the edges of $\bar{G}$ are drawn based on the entries in $J(\cdot)$. If, independent of the argument of $J(\cdot)$, $[J(\cdot)]_{ij} \leq 0$ for $i \neq j$, then we draw an edge from node j to node i labeled with a "−" sign; if, independent of the argument of $J(\cdot)$, $[J(\cdot)]_{ij} \geq 0$ for $i \neq j$, then we draw an edge labeled with a "+" sign. If $[J(\cdot)]_{ij} \leq 0$ for some argument, and $[J(\cdot)]_{ij} \geq 0$ for some other argument then from node j to node i we draw an edge labeled with a "−" sign, and also an edge labeled with a "+" sign. Furthermore, if from node j to node i, there are edges with a "−" sign and with a "+" sign, then we introduce a node between i and j, say i' such that there is an edge with a "+" sign from i to i'; an edge with "+" sign from i' to j; the edge with a "−" sign from j to i is retained; see (Sontag, 2007, Figure 3). We refer to the graph constructed with the addition of such nodes as $\hat{G}$. Thus, $\hat{G}$ is a signed graph. Note that $\hat{G}$ has no self-loops.

We will also be requiring the following notion from graph theory. A signed graph is said to be consistent if every undirected cycle in the graph has a net positive sign, i.e., it has an even number of "−" signs (Sontag, 2007).

7.2. The coupled bivirus system is not monotone

We now show that the coupled bivirus system is not monotone.

Theorem 4. *Under Assumptions 1 and 2, system (8)–(10) is not monotone.*

Proof. First, note that the Jacobian $J(x^{(1)}, x^{(2)}, z)$, as in (15), has $3n$ rows and $3n$ columns. Hence, the graph $\bar{G}$, constructed with respect to the Jacobian in (15), has $3n$ nodes. Next, observe that the 12 and 21 blocks of $J(x^{(1)}, x^{(2)}, z)$ are, due to Assumptions 1 and 2, negative matrices, which implies that for any node i, the edge from node i (resp. $i + n$) to node $i + n$ (resp. i) has a "−" sign. Similarly, the 31 and 32 blocks of $J(x^{(1)}, x^{(2)}, z)$ are, due to Assumptions 1 and 2, positive matrices, which implies that for any node i, the edge from node i (resp. $i + n$) to node $i + 2n$ has a "+" sign.

Note that the 13 block of $J(x^{(1)}, x^{(2)}, z)$ can change its sign depending on the argument. Hence, it is clear that, for any node i, there is an edge from node $i + 2n$ to i with a "−" sign, and an edge with a "+" sign. Therefore, we introduce n additional nodes, and label these $3n + 1$, $3n + 2 \ldots 4n$. Similarly, since the 23 block of $J(x^{(1)}, x^{(2)}, z)$ can change its sign depending on the argument, it follows that for any node i, there is an edge from node $i + 2n$ to $i + n$ with a "−" sign, and an edge with "+" sign. Therefore, we introduce further n additional nodes, and label those $4n + 1$, $4n+2 \ldots 5n$. The edges corresponding to the nodes labeled $3n+1$, $3n + 2 \ldots 4n$, and $4n + 1, 4n + 2, \ldots 5n$ are assigned as outlined in Section 7.1; thus obtaining the corresponding graph $\hat{G}$.

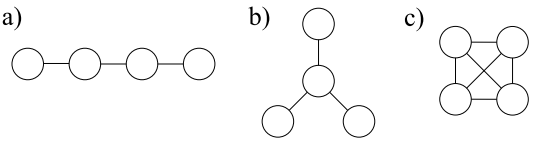

Fig. 2. Graph structures: (a) line, (b) star, (c) complete.

In graph $\hat{G}$, the loop starting from node i traversing through node $i + 3n$, node $i + 2n$, node $i + n$ and back to node i is a 4-length cycle that has an odd number (namely, one) of negative signs. Therefore, from (Sontag, 2007, page 62), the signed graph $\hat{G}$ is not consistent. Consequently, from (Sontag, 2007, page 63), it follows that the system (8)–(10) is not monotone. ■

Theorem 4 answers Question (viii) raised in Section 3.1. Furthermore, Theorem 4 implies that we cannot leverage the rich literature on monotone dynamical systems (Hirsch, 1988; Smith, 1988) to study the limiting behavior of system (8)–(10). In general, for non-monotone systems, no dynamical behavior, including chaos, can be definitively ruled out (Sontag, 2007). Therefore, novel tools are needed to study coupled bivirus systems more in-depth. The development of such tools is beyond the scope of this paper.

8. Simulations

This section presents a comparison of the 4^n-state Markov process in (1)–(4) to (8)–(10) via simulation, and also provides a set of simulations of various coupled virus models.

8.1. Comparison to full probabilistic model

We compare the model in (8)–(10) to the full probabilistic 4^n-state model in (1)–(4) via simulations to illustrate the effectiveness of the approximation. We set $\epsilon^{(1)} = \epsilon^{(2)} = 3$, and use line graphs, star (hub–spoke) graphs, and complete graphs. For examples of each type of graph, see Fig. 2. All adjacency matrices for these graphs are symmetric and binary-valued, and both viruses spread over the same graph. In the star graph, the central node is the first agent. Each simulation was run for 10,000 time steps (final time $T = 10{,}000$), with three initial conditions: (1) the first node is infected by virus 1 and the second node is infected by virus 2,

$$\begin{aligned} x^{(1)}(0) &= [1\ 0\ \cdots\ 0]^\top \\ x^{(2)}(0) &= [0\ 1\ 0\ \cdots\ 0]^\top \\ z(0) &= \mathbf{0}; \end{aligned} \tag{20}$$

(2) the first node is infected by virus 1, the second node is infected by virus 2, and the third node is infected by both virus 1 and virus 2,

$$\begin{aligned} x^{(1)}(0) &= [1\ 0\ \cdots\ 0]^\top \\ x^{(2)}(0) &= [0\ 1\ 0\ \cdots\ 0]^\top \\ z(0) &= [0\ 0\ 1\ 0\ \cdots\ 0]^\top; \end{aligned} \tag{21}$$

and (3) the first node is infected by virus 1, the second node is infected by virus 2, and the remaining nodes are infected by both virus 1 and virus 2,

$$\begin{aligned} x^{(1)}(0) &= [1\ 0\ \cdots\ 0]^\top \\ x^{(2)}(0) &= [0\ 1\ 0\ \cdots\ 0]^\top \\ z(0) &= [0\ 0\ 1\ \cdots\ 1]^\top. \end{aligned} \tag{22}$$

In these tests we explore identical homogeneous viruses, $(\beta, \delta) = (\beta^{(1)}, \delta^{(1)}) = (\beta^{(2)}, \delta^{(2)}) = (\beta^{(3)}, \delta^{(3)})$. The (β, δ) pairs are

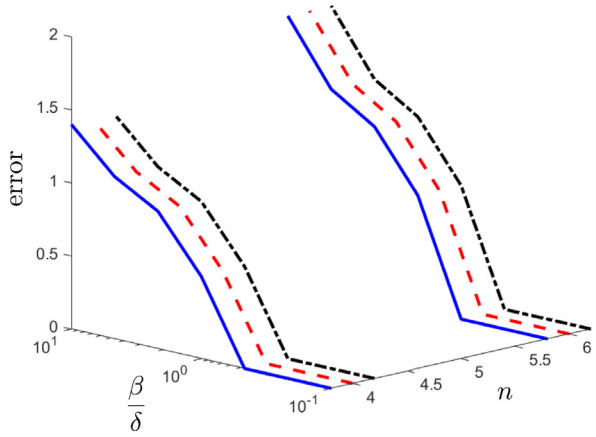

Fig. 3. A plot of $\|[v^{(1)}(T); v^{(2)}(T); v^{(3)}(T)] - [x^{(1)}(T); x^{(2)}(T); z(T)]\|$ for the line graph, $T = 10{,}000$. Results from using the different initial conditions (20), (21), and (22) are depicted by the blue lines, red dashed lines, and black dash-dot lines, respectively. (For interpretation of the references to color in this figure legend, the reader is referred to the web version of this article.)

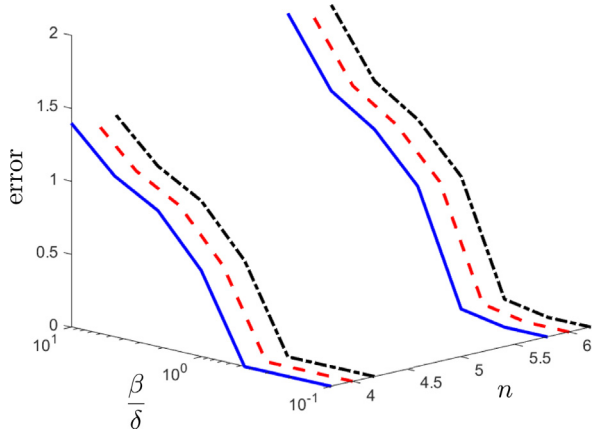

Fig. 4. A plot of $\|[v^{(1)}(T); v^{(2)}(T); v^{(3)}(T)] - [x^{(1)}(T); x^{(2)}(T); z(T)]\|$ for the star graph, $T = 10{,}000$. Results from using the different initial conditions (20), (21), and (22) are depicted by the blue lines, red dashed lines, and black dash-dot lines, respectively. (For interpretation of the references to color in this figure legend, the reader is referred to the web version of this article.)

$[(0.1, 1), (0.215, 1), (0.464, 1), (0.5, 0.5), (1, 0.464), \quad (1, 0.215), (1, 0.1)]$, and the numbers of agents are $n = 4, 6$. We limited simulations to these n values since mean field approximations are typically worse for small values of n and there is a computational limitation due to the size of the 4^n-state Markov model.

The results are given in Figs. 3–5 in terms of the 2-norm of the difference between the states of (8)–(10) at the final time ($[x^{(1)}(T); x^{(2)}(T); z(T)]$), and the means of the three states in the 4^n-state Markov model at the final time ($[v^{(1)}(T); v^{(2)}(T); v^{(3)}(T)]$ as defined by (4)). The accuracy of the approximation appears to be very similar to the single virus case (Van Mieghem et al., 2009) and to the two-virus case (Liu et al., 2019). Since the model in (8)–(10) is an upper bounding approximation, the results show that the two models converge to the healthy state for the smaller values of $\frac{\beta}{\delta}$, resulting in small errors between the two models. For many of the larger values of $\frac{\beta}{\delta}$, the model in (8)–(10) again performs quite well since it is at an epidemic state and the 4^n-state Markov model does not appear to reach the healthy state in the finite time considered in the simulations ($T = 10{,}000$). Therefore, for certain values of $\frac{\beta}{\delta}$ and certain time scales, the model in (8)–(10) is a sufficient approximation of the 4^n-state Markov model. For values of $\frac{\beta}{\delta}$ that are near 1, the models are quite different, similar to the single- and bi-virus cases. The 4^n-state Markov model appears, in most cases, to be at or close to the healthy state while the model in (8)–(10) is at an epidemic state, resulting in large errors.

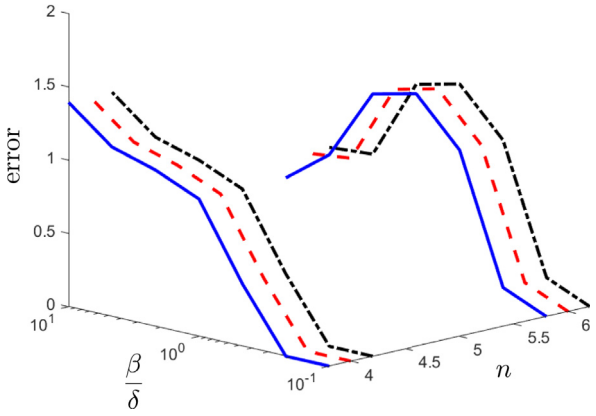

Fig. 5. A plot of the error $\|[v^1(T); v^2(T); v^3(T)] - [x^{(1)}(T); x^{(2)}(T); z(T)]\|$ for the complete graph, $T = 10{,}000$. Results from using the different initial conditions (20), (21), and (22) are depicted by the blue lines, red dashed lines, and black dash-dot lines, respectively. (For interpretation of the references to color in this figure legend, the reader is referred to the web version of this article.)

8.2. Illustrative examples

Virus 1 is depicted by the color red (r), virus 2 is depicted by the color blue (b), and the state of being infected with both states, $z(t)$, is depicted by the color green (g). For all $i \in [n]$, the color at each time t for node i is given by

$$\frac{x_i^{(1)}(t)}{s_i(t)}r + \frac{x_i^{(2)}(t)}{s_i(t)}b + \frac{z_i(t)}{s_i(t)}g, \tag{23}$$

where $s_i(t) = x_i^{(1)}(t) + x_i^{(2)}(t) + z_i(t)$. When $x_i^{(1)}(t) + x_i^{(2)}(t) + z_i(t) = 0$, the color is black, indicating completely healthy, susceptible. These color variations are used to facilitate the depiction of the parallel equilibria ($\hat{x}^{(1)} = \alpha\hat{x}^{(2)}$), a behavior that is exhibited by the $\epsilon^{(1)} = \epsilon^{(2)} = 0$ case (see Liu et al. 2016) and are illustrated by all the nodes converging to the same color. For all $i \in [n]$, the diameter of node i is given by

$$d_0 + s_i(t)r_0, \tag{24}$$

with d_0 being the default/smallest diameter and r_0 being the scaling factor depending on the total sickness of node i. Therefore, the color indicates the type of virus(es) each agent has and the diameter indicates the degree of sickness for each agent. The graph structure is as follows:

$$a_{ij}(t) = \begin{cases} e^{-\|y_i(t) - y_j(t)\|^2}, & \text{if } \|z_i(t) - z_j(t)\| < \hat{r}, \\ 0, & \text{otherwise}, \end{cases} \tag{25}$$

where $y_i(t) \in \mathbb{R}^2$ is the position of node i, with $\hat{r} = .35$.

We consider a network of $n = 15$ nodes. The binary matrices $A^{(1)}$ and $A^{(2)}$ are populated in correspondence, respectively, to the black and green edges depicted in Fig. 6. The initial condition of the network is shown in Fig. 6. The elements of diagonal matrices $D^{(1)}$ and $D^{(2)}$ are chosen uniformly at random from $[0, 1]$. Let $b^{(1)}$ be a vector whose elements are chosen uniformly at random from $[0, 1]$. Let $B^{(1)} = \text{diag}(B^{(1)}/6)A^{(1)}$. Vector $b^{(2)}$ is chosen analogous to $b^{(1)}$. Then, let $B^{(2)} = \text{diag}(b^{(2)}/11)A^{(2)}$. Let $\epsilon^{(1)} = \epsilon^{(2)} = \epsilon$, and fix $\epsilon = 0.5$. Given that the matrices involved are of dimension

15×15, in the interest of space, we refrain from providing exact values; the exact values used along with the MATLAB code used are available via github.[4] With these choices of model parameters, it turns out that $s(-D^{(1)} + B^{(1)}) = -0.0037 < 0$ and $s(-D^{(2)} + B^{(2)}) = -0.0013 < 0$. Consistent with Proposition 1 (and since $\epsilon \in (0, 1)$, also consistent with Theorem 1), both the viruses die out; see Fig. 7(a). Next, with the same model parameters and initial condition as before, we set $\epsilon = 2$. Again, consistent with Proposition 1, the dynamics converge to the healthy state, albeit the rate of convergence is slower than that with $\epsilon = 0.5$; see Fig. 7(b). Once again, with the same model parameters and initial condition as before, we set $\epsilon = 1000$. Although $s(-D^{(1)} + B^{(1)}) = -0.0037 < 0$ and $s(-D^{(2)} + B^{(2)}) = -0.0013 < 0$, as a consequence of the effect of the large value of ϵ, the dynamics do not die out; see Fig. 8. Next, using the same set of parameters as for the simulations in Fig. 7(a), except for $\epsilon^{(1)} = 2$ and $\epsilon^2 = 0.5$, we check the conditions in Proposition 1. It seems that, although it needs to be proven rigorously, even with the aforementioned choice of $\epsilon^{(m)}$ for $m = 1, 2$, the conditions in Proposition 1 guarantee eradication of both the viruses; see Fig. 9.

For the next simulation, $D^{(1)}$, $D^{(2)}$, $b^{(1)}$, and $b^{(2)}$ are the same as before. Let $B^{(1)} = \text{diag}(b^{(1)})A^{(1)}$, and let $B^{(2)} = \text{diag}(b^{(2)}/11)A^{(2)}$. Choose $\epsilon = 0.5$. With these choices of model parameters, it turns out that $s(-D^{(1)} + B^{(1)}) = 1.4904 > 0$ and $s(-D^{(2)} + B^{(2)}) = -0.0013 < 0$. Consistent with Theorem 2, virus 2 dies out, virus 1 becomes endemic in the population, and no fraction of any node is infected by both viruses 1 and 2 simultaneously; see Fig. 10.

Next, $D^{(1)}$, $D^{(2)}$, $b^{(1)}$, and $b^{(2)}$ take the same values as before. Let $B^{(1)} = \text{diag}(b^{(1)}/2)A^{(1)}$, and let $B^{(2)} = \text{diag}(b^{(2)}/10)A^{(2)}$. We choose $\epsilon = 0.5$. With such a choice, we obtain $s(-D^{(1)}+B^{(1)}) = 0.5026 > 0$, thus ensuring the existence of an endemic equilibrium $\hat{x}^{(1)}$. We also have $s(-D^{(2)} + B^{(2)}) = 0.0063$. Further, we have that $s(-D^{(2)} + (I - \hat{X}^{(1)})B^{(2)}) = -0.0210 < 0$, and $s\Big((-D^{(1)} - D^{(2)} + \epsilon\hat{X}^{(1)}B^{(2)}) - (\epsilon\hat{B}^{(1)} + \epsilon\hat{X}^{(1)}B^{(2)})(-D^{(2)} + (I - \hat{X}^{(1)})B^{(2)} - \epsilon\hat{B}^{(1)})^{-1}((I - \hat{X}^{(1)})B^{(2)} + D^{(1)})\Big) = -0.0259 < 0$. Hence, in line with the result in Theorem 3, the dynamics converge to $(\hat{x}^{(1)}, \mathbf{0}, \mathbf{0})$ exponentially fast; see Fig. 11.

Note that we also ran the same set of simulations on a large-scale network, namely the graph of adjacent counties in the contiguous United States of America ($n = 3109$). We used the same adjacency matrix as in (Paré, Liu, et al., 2020), with practically identical outcomes on the average infection levels; see (Gracy et al., 2024, Section 8.3) for more details.

9. Conclusion

We have addressed the problem of simultaneous infection of an individual (resp. subpopulation) by possibly two viruses. We derived a coupled bi-virus model from a 4^n-state Markov process. We identified a condition that leads to the extinction of both viruses; likewise a condition that causes one of the viruses to become endemic in the population. Subsequently, we provided a sufficient condition and two necessary conditions for local exponential convergence of boundary equilibria. With respect to coexistence equilibria, we conclusively ruled out the existence of the following types of coexisting equilibria: (i) a point in the state space where for each node there is a non-trivial fraction infected only by virus 1, a non-trivial fraction infected only by virus 2, but no fraction that is infected by both viruses 1 and 2; and (ii) a point in the state space where for each node there is a fraction that is infected simultaneously by both viruses 1 and 2, but no

[4] https://github.com/philpare/coupled_bivirus

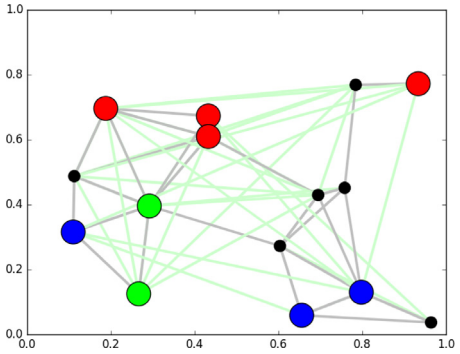

Fig. 6. Initial condition of the network. Black: healthy nodes; red: nodes infected only by virus 1; blue: nodes infected only by virus 2; and green: nodes infected by both viruses 1 and 2. Black edges: spreading pattern for virus 1; green edges: spreading pattern for virus 2. (For interpretation of the references to color in this figure legend, the reader is referred to the web version of this article.)

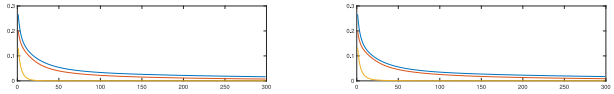

(a) With $\epsilon = 0.5$ (b) With $\epsilon = 2$

Fig. 7. In both figures, the red line indicates the average infection level of the population with respect to virus 1; the blue line with respect to virus 2; and the yellow line with respect to both viruses 1 and 2. (For interpretation of the references to color in this figure legend, the reader is referred to the web version of this article.)

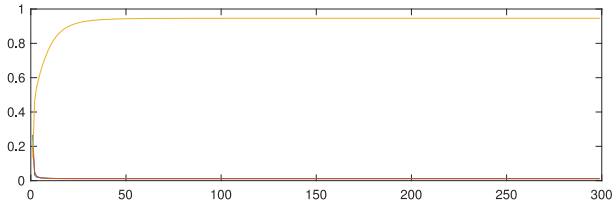

Fig. 8. The parameters chosen fulfill the conditions in Proposition 1, but since $\epsilon(= 1000)$ is quite large the dynamics do not converge to the healthy state.

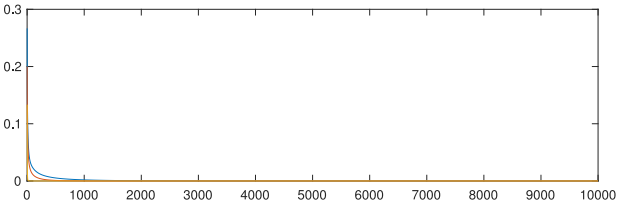

Fig. 9. The parameters are chosen so as to fulfill the conditions in Proposition 1, with the exception that $\epsilon^{(1)} = 0.5$ and $\epsilon^{(2)} = 2$. The dynamics still converge to the healthy state.

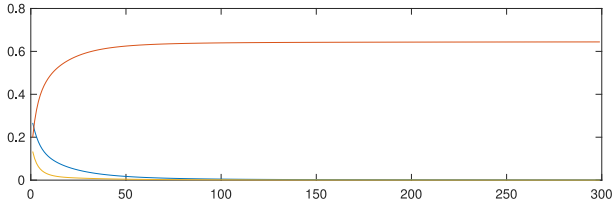

Fig. 10. Virus 1 becomes endemic; virus 2 has died out completely, and no fraction of any node is infected by both viruses 1 and 2.

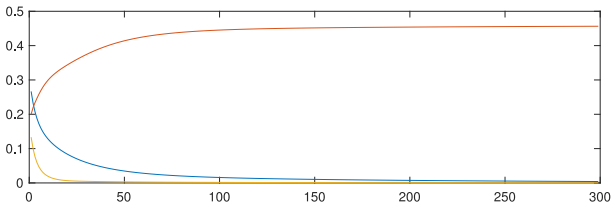

Fig. 11. Average infection level with respect to virus 1, virus 2, and virus 1 and virus 2 using the initial condition in Fig. 6.

fraction is infected only by virus 1 (resp. virus 2). We provided a necessary condition for the existence of certain other kinds of coexisting equilibria. Finally, we showed that the coupled bi-virus model is not monotone.

The fact that the coupled bivirus system is not monotone makes its stability analysis harder. However, one could leverage the theory of singular perturbations for monotone systems (Wang & Sontag, 2006) to possibly draw conclusions on the generic convergence of the coupled bivirus system, whereas one could possibly take recourse to the Lyapunov techniques espoused in (Shuai & van den Driessche, 2013) to establish global asymptotic stability of boundary equilibria. Other problems of further interest include identifying condition(s) for stability (local or global) of various coexisting equilibria.

Acknowledgments

We thank Prof. Wendy Anne Beauvais (Department of Comparative Pathobiology, College of Veterinary Medicine, Purdue University) for discussions regarding co-infection in animal populations that have contributed to the design of our model. We also thank the anonymous reviewers whose feedback has improved the paper.

Appendix

Proof of Theorem 1. Let $y_i^{(1)}(t) = x_i^{(1)}(t) + z_i(t)$ and $y_i^{(2)}(t) = x_i^{(2)}(t) + z_i(t)$ for each $i \in [n]$. From (5)–(7), the dynamics of $y_i^{(1)}(t)$ and $y_i^{(2)}(t)$ are

$$\begin{aligned}\dot{y}_i^{(1)}(t) &= -\delta_i^{(1)} y_i^{(1)}(t) + (1 - y_i^{(1)}(t) - (1-\epsilon^{(2)}) x_i^{(2)}(t)) \textstyle\sum_{j=1}^n \beta_{ij}^{(1)} y_j^1(t),\\ \dot{y}_i^{(2)}(t) &= -\delta_i^{(2)} y_i^{(2)}(t) + (1 - y_i^{(2)}(t) - (1-\epsilon^{(1)}) x_i^{(1)}(t)) \textstyle\sum_{j=1}^n \beta_{ij}^{(2)} y_j^{(2)}(t).\end{aligned} \tag{26}$$

Since $\epsilon^{(1)}, \epsilon^{(2)} \in [0, 1]$, it follows that

$$\begin{aligned}\dot{y}_i^{(1)}(t) &\le -\delta_i^{(1)} y_i^{(1)}(t) + (1 - y_i^{(1)}(t)) \textstyle\sum_{j=1}^n \beta_{ij}^{(1)} y_j^{(1)}(t),\\ \dot{y}_i^{(2)}(t) &\le -\delta_i^{(2)} y_i^{(2)}(t) + (1 - y_i^{(2)}(t)) \textstyle\sum_{j=1}^n \beta_{ij}^{(2)} y_j^{(2)}(t),\end{aligned}$$

which implies that the trajectories of $y_i^{(1)}(t)$ and $y_i^{(2)}(t)$ in (26) are both bounded above by the trajectory of a single-virus SIS model. From (Liu et al., 2016, Proposition 3), in the case when $s(B^{(1)} - D^{(1)}) \le 0$ and $s(B^{(2)} - D^{(2)}) \le 0$, then all $y_i^{(1)}(t)$ and $y_i^{(2)}(t)$ asymptotically converge to 0 for any initial condition, which implies that system (8)–(10) asymptotically converges to the healthy state for any initial state in $\mathcal{D}$. Therefore, the healthy state is the unique equilibrium of the system.

Proof of Theorem 2. Let $y_i^{(2)}(t) = x_i^{(2)}(t) + z_i(t)$ for each $i \in [n]$. From the proof of Theorem 1, since $s(B^{(2)} - D^{(2)}) \le 0$ and $\epsilon^{(1)} \in [0, 1]$, all $y_i^{(2)}(t)$ converge to zero, which implies all $x_i^{(2)}(t)$ and $z_i(t)$ converge to zero as well. From (5), the dynamics of all $x_i^{(1)}(t)$, $i \in [n]$ can be viewed as a cascade system with $x_i^{(2)}(t)$, $z_i(t)$, $i \in [n]$ as inputs. Using similar arguments to those in the proof of (Khanafer et al., 2016, Theorem 4), this cascade system is input-to-state stable. Note that with $x_i^{(2)}(t) = z_i(t) = 0$ for all $i \in [n]$, the dynamics of all $x_i^{(1)}(t)$ in (5) simplify to the single-virus networked SIS model. The theorem is then a direct consequence of (Khalil, 2002, Lemma 4.7) and (Liu et al., 2019, Proposition 3).

Proof of Corollary 2. Consider system (8)–(10). Note that, by the definition of equilibrium, the healthy state $(\mathbf{0}, \mathbf{0}, \mathbf{0})$ is an equilibrium point, regardless of whether (or not), for $m \in [2]$, $s(B^{(m)} - D^{(m)}) \le 0$. Since, by assumption, for $m \in [2]$, $s(B^{(m)} - D^{(m)}) > 0$, instability of $(\mathbf{0}, \mathbf{0}, \mathbf{0})$ follows from the proof of Proposition 1. The existence and uniqueness of the equilibrium points $(\hat{x}^{(1)}, \mathbf{0}, \mathbf{0})$ and $(\mathbf{0}, \hat{x}^{(2)}, \mathbf{0})$ follow from the proof of Theorem 2.

We need the following lemmas to prove Theorem 3.

Lemma 2 (*Varga 1999, Lemma 2.3*)**.** *Suppose that M is an irreducible Metzler matrix. Then $r = s(M)$ is a simple eigenvalue of M, and if $M\zeta = r\zeta$, then $\zeta \gg \mathbf{0}$.*

Lemma 3. *Consider system (8)–(10) under Assumption 1 and 3. If $(\hat{x}^{(1)}, \hat{x}^{(2)}, \hat{z}) \in \mathcal{D}$ such that $\hat{x}^{(1)}, \hat{x}^{(2)}, \hat{z} > \mathbf{0}$, then $\mathbf{0} \ll \hat{x}^{(1)} \ll \mathbf{1}$ or $\mathbf{0} \ll \hat{x}^{(2)} \ll \mathbf{1}$ or $\mathbf{0} \ll \hat{z} \ll \mathbf{1}$. Furthermore, $\hat{x}^{(1)} + \hat{x}^{(2)} + \hat{z} \ll \mathbf{1}$.*

Proof. See the proof of (Gracy et al., 2024, Lemma 6).

Lemma 4 (*Souza, Wirth, and Shorten 2017, Corollary 1*)**.** *Let $A \in \mathbb{R}^{n\times n}$ be a Metzler matrix partitioned in blocks as*

$$A = \begin{bmatrix} A_{11} & A_{12} \\ A_{21} & A_{22} \end{bmatrix}$$

in which A_{11} and A_{22} are square matrices. Define $A/A_{11} := A_{22} - A_{21}A_{11}^{-1}A_{12}$. Then, A is Hurwitz if, and only if, A_{11} and A/A_{11} are Hurwitz Metzler matrices.

Proof of Theorem 3. Consider the equilibrium point $(\hat{x}^{(1)}, \mathbf{0}, \mathbf{0})$. The Jacobian matrix of this equilibrium point can be rewritten as

$$J(\hat{x}^{(1)}, \mathbf{0}, \mathbf{0}) = \begin{bmatrix} -D^{(1)} + (I - \hat{X}^{(1)})B^{(1)} - \hat{B}^{(1)} & \hat{J} \\ \mathbf{0} & \tilde{J} \end{bmatrix}. \tag{27}$$

where $\hat{J} = [\, -\hat{B}^{(1)} - \epsilon\hat{X}^{(1)}B^{(2)} \quad D^{(2)} - \hat{B}^{(1)} + (I - \hat{X}^{(1)})B^{(1)} - \epsilon\hat{X}^{(1)}B^{(2)} \,]$, while

$$\tilde{J} = \begin{bmatrix} -D^{(2)} + (I - \hat{X}^{(1)})B^{(2)} - \epsilon\hat{B}^{(1)} & (I - \hat{X}^{(1)})B^{(2)} + D^{(1)} \\ \epsilon\hat{B}^{(1)} + \epsilon\hat{X}^{(1)}B^{(2)} & -D^{(1)} - D^{(2)} + \epsilon\hat{X}^{(1)}B^{(2)} \end{bmatrix}. \tag{28}$$

From (27) it is clear that the matrix $J(\hat{x}^{(1)}, \mathbf{0}, \mathbf{0})$ is block upper triangular. Therefore, $s(J(\hat{x}^{(1)}, \mathbf{0}, \mathbf{0})) < 0$ if, and only if, the following conditions are satisfied: (i) $s(-D^{(1)} + (I - \hat{X}^{(1)})B^{(1)} - \hat{B}^{(1)}) < 0$, and (ii) $s(\tilde{J}) < 0$. Since $(\hat{x}^{(1)}, \mathbf{0}, \mathbf{0})$ is an equilibrium point, from (8) we obtain:

$$(-D^{(1)} + (I - \hat{X}^{(1)})B^{(1)})\hat{x}^{(1)} = \mathbf{0}. \tag{29}$$

Define $Q := D^{(1)} - (I - \hat{X}^{(1)})B^{(1)}$. Since $-Q$ is an irreducible Metzler matrix, and since $\hat{x}^{(1)} \gg \mathbf{0}$, applying Lemma 2 to (29) yields $s(-Q) = 0$. Note that $-Q$ being Metzler implies that Q is an M-matrix, and since $s(-Q) = 0$ it follows that Q is an irreducible singular M-matrix. Since $B^{(1)}$ is nonnegative irreducible, and $\hat{x}^{(1)} \gg \mathbf{0}$, it follows that the matrix $\hat{B}^{(1)}$ has at least one diagonal element that is strictly positive. Therefore, due to (Qu, 2009, Corollary 4.33), the matrix $Q + \hat{B}^{(1)}$ is a non-singular M-matrix, which further implies that $s(-D^{(1)} + (I - \hat{X}^{(1)})B^{(1)} - \hat{B}^{(1)}) < 0$.

From (28), it is immediate that $\tilde{J}$ is Metzler. We now prove, by using Lemma 4, that the matrix $\tilde{J}$ is also Hurwitz. Observe that

$\tilde{J}_{11} = -D^{(2)} + (I - \hat{X}^{(1)})B^{(2)} - \epsilon\hat{B}^{(1)}$. Since by Lemma 3, $\hat{x}^{(1)} \ll \mathbf{1}$, it follows that $(I - \hat{X}^{(1)})$ is a positive diagonal matrix. Since by Assumption 2, $B^{(2)}$ is nonnegative irreducible, it is clear that $(I - \hat{X}^{(1)})B^{(2)}$ is nonnegative irreducible, and hence $\tilde{J}_{11}$ is Metzler. By assumption, $s(-D^{(2)}+(I-\hat{X}^{(1)})B^{(2)}) < 0$. Hence, by using similar arguments involved in showing that $s(-D^{(1)}+(I-\hat{X}^{(1)})B^{(1)}-\hat{B}^{(1)}) < 0$, we can also show that $s(\tilde{J}_{11}) < 0$. Therefore, $\tilde{J}_{11}$ is a Hurwitz Metzler matrix.

Note that

$$\begin{aligned}\tilde{J}/\tilde{J}_{11} =&(-D^{(1)} - D^{(2)} + \epsilon\hat{X}^{(1)}B^{(2)})\\ &- (\epsilon\hat{B}^{(1)} + \epsilon\hat{X}^{(1)}B^{(2)})(-D^{(2)} + (I - \hat{X}^{(1)})B^{(2)}\\ &- \epsilon\hat{B}^{(1)})^{-1}((I - \hat{X}^{(1)})B^{(2)} + D^{(1)}).\end{aligned}$$

Note that the existence of $(-D^{(2)} + (I - \hat{X}^{(1)})B^{(2)} - \epsilon\hat{B}^{(1)})^{-1}$ is a consequence of Hurwitzness of $(-D^{(2)} + (I - \hat{X}^{(1)})B^{(2)} - \epsilon\hat{B}^{(1)})$ (Berman & Plemmons, 1994; Briat, 2017). Furthermore, observe that since $(-D^{(2)} + (I - \hat{X}^{(1)})B^{(2)} - \epsilon\hat{B}^{(1)})^{-1}$ is Metzler, it follows that $-(-D^{(2)} + (I - \hat{X}^{(1)})B^{(2)} - \epsilon\hat{B}^{(1)})^{-1}$ is an M-matrix. Since $-(-D^{(2)} + (I - \hat{X}^{(1)})B^{(2)} - \epsilon\hat{B}^{(1)})^{-1}$ exists, it follows that $-(-D^{(2)} + (I - \hat{X}^{(1)})B^{(2)} - \epsilon\hat{B}^{(1)})^{-1}$ is a nonsingular M-matrix. Hence, $-(-D^{(2)}+(I-\hat{X}^{(1)})B^{(2)}-\epsilon\hat{B}^{(1)})^{-1}$ is a nonnegative matrix (Plemmons, 1977, F.15). Define

$$\begin{aligned}Q_1 :=& -(\epsilon\hat{B}^{(1)} + \epsilon\hat{X}^{(1)}B^{(2)})\times\\ &(-D^{(2)} + (I - \hat{X}^{(1)})B^{(2)} - \epsilon\hat{B}^{(1)})^{-1}((I - \hat{X}^{(1)})B^{(2)} + D^{(1)}).\end{aligned}$$

Since $\epsilon \geq 0$, from Assumption 3 it is clear that $\hat{B}^{(1)}$ is nonnegative diagonal matrix, $B^{(2)}$ is nonnegative, and $D^{(1)}$ and $D^{(2)}$ are positive diagonal matrices. Hence, since from Lemma 3 the matrix $(I-\hat{X}^{(1)})$ is also positive, it is immediate that Q_1 is nonnegative. Therefore, since $(-D^{(1)}-D^{(2)}+\epsilon\hat{X}^{(1)}B^{(2)})$ is Metzler, it follows that the matrix $(-D^{(1)} - D^{(2)} + \epsilon\hat{X}^{(1)}B^{(2)}) + Q_1$ is Metzler. Consequently, $\tilde{J}/\tilde{J}_{11}$ is Metzler. Since, by assumption, $s\Big((-D^{(1)}-D^{(2)}+\epsilon\hat{X}^{(1)}B^{(2)})-(\epsilon\hat{B}^{(1)}+\epsilon\hat{X}^{(1)}B^{(2)})(-D^{(2)}+(I-\hat{X}^{(1)})B^{(2)}-\epsilon\hat{B}^{(1)})^{-1}((I-\hat{X}^{(1)})B^{(2)}+D^{(1)})\Big) < 0$, it means that $s((-D^{(1)}-D^{(2)}+\epsilon\hat{X}^{(1)}B^{(2)})+Q_1) < 0$, thereby implying that $s(\tilde{J}/\tilde{J}_{11}) < 0$. Thus, $\tilde{J}/\tilde{J}_{11}$ is Hurwitz Metzler. Therefore, from Lemma 4, it follows that the matrix $\tilde{J}$ is Hurwitz. Hence, we can conclude that $s(J(\hat{x}^{(1)}, \mathbf{0}, \mathbf{0})) < 0$. Local exponential stability of $(\hat{x}^{(1)}, \mathbf{0}, \mathbf{0})$ then follows from (Khalil, 2002, Theorem 4.15 and Corollary 4.3), thus concluding the proof. ■

Proof of Proposition 2. Consider the matrix $\tilde{J}$ given in (28). Suppose that $s(-D^{(2)}+(I-\hat{X}^{(1)})B^{(2)}-\epsilon\hat{B}^{(1)}) \geq 0$. This implies that $[\tilde{J}]_{11}$ (i.e., the 11-block of $\tilde{J}$) is not Hurwitz. Hence, from Lemma 4, it follows that $\tilde{J}$ is not Hurwitz. That is, $s(\tilde{J}) \geq 0$. Therefore, it follows that $J(\hat{x}^{(1)}, \mathbf{0}, \mathbf{0})$ is not Hurwitz, and, consequently, the equilibrium point $(\hat{x}^{(1)}, \mathbf{0}, \mathbf{0})$ is not locally exponentially stable.

Note that if $s\Big((-D^{(1)} - D^{(2)} + \epsilon\hat{X}^{(1)}B^{(2)}) - (\epsilon\hat{B}^{(1)} + \epsilon\hat{X}^{(1)}B^{(2)})(-D^{(2)} + (I - \hat{X}^{(1)})B^{(2)} - \epsilon\hat{B}^{(1)})^{-1}((I - \hat{X}^{(1)})B^{(2)} + D^{(1)})\Big) \geq 0$, then the matrix $\tilde{J}/\tilde{J}_{11}$ is not Hurwitz. The rest of the proof is analogous to that of necessity of item (i). ■

Proof of Corollary 3. Assume that $s(-D^1 - D^2 + \epsilon\hat{x}^{(1)}B^{(2)}) > 0$. Note that, from the proof of Theorem 3, $(-D^1 - D^2 + \epsilon\hat{x}^{(1)}B^{(2)}) < \tilde{J}/\tilde{J}_{11}$, where $\tilde{J}/\tilde{J}_{11}$ is as given in the proof of Theorem 3. Since both $(-D^1 - D^2 + \epsilon\hat{x}^{(1)}B^{(2)})$ and $\tilde{J}/\tilde{J}_{11}$ are Metzler matrices, due to the assumption that $s(-D^1 - D^2 + \epsilon\hat{x}^{(1)}B^{(2)}) > 0$, it follows from (Varga, 2009, Theorem 2.1) that $s(\tilde{J}/\tilde{J}_{11}) > 0$. Consequently, it follows from Lemma 4 that the matrix J in (28) is not Hurwitz. Hence, $s(J(\hat{x}^{(1)}, \mathbf{0}, \mathbf{0})) > 0$, which further implies from (Khalil, 2002, Theorem 4.7) that the boundary equilibrium $(\hat{x}^{(1)}, \mathbf{0}, \mathbf{0})$ is unstable. ■

Proof of Proposition 3. Suppose, to the contrary, that there exists an equilibrium of the form $(\hat{x}^{(1)}, \hat{x}^{(2)}, \mathbf{0})$ with $\hat{x}^{(1)}, \hat{x}^{(2)} > \mathbf{0}$ for system (8)–(10). By assumption $(\hat{x}^{(1)}, \hat{x}^{(2)}, \mathbf{0})$ is a non-zero equilibrium point. Hence, from Lemma 3, it follows that $\mathbf{0} \ll \hat{x}^{(1)}$ and $\mathbf{0} \ll \hat{x}^{(2)}$. Since $(\hat{x}^{(1)}, \hat{x}^{(2)}, \mathbf{0})$ is an equilibrium point, the equilibrium version of Eq. (10) reads as follows:

$$\mathbf{0} = \epsilon^{(1)}\hat{x}^{(1)}B^{(2)}\hat{x}^{(2)} + \epsilon^{(2)}\hat{x}^{(2)}B^{(1)}\hat{x}^{(1)}. \tag{30}$$

Note that, by assumption, $\epsilon^{(m)} > 0$ for some $m \in [2]$. By Assumption 2, the matrices $B^{(1)}$ and $B^{(2)}$ are nonnegative irreducible, thus, since $\hat{x}^{(1)}$ and $\hat{x}^{(2)}$ are strictly positive vectors, implying that either $\epsilon^{(1)}\hat{x}^{(1)}B^{(2)}\hat{x}^{(2)} > \mathbf{0}$ or $\epsilon^{(2)}\hat{x}^{(2)}B^{(1)}\hat{x}^{(1)} > \mathbf{0}$. As a consequence, $\epsilon^{(1)}\hat{x}^{(1)}B^{(2)}\hat{x}^{(2)} + \epsilon^{(2)}\hat{x}^{(2)}B^{(1)}\hat{x}^{(1)} > 0$, which contradicts (30). Therefore, there does not exist a coexisting equilibrium of the form $(\hat{x}^{(1)}, \hat{x}^{(2)}, \mathbf{0})$ with $\hat{x}^{(1)}, \hat{x}^{(2)} > \mathbf{0}$. ■

References

Ahn, Y.-Y., Jeong, H., Masuda, N., & Noh, J. D. (2006). Epidemic dynamics of two species of interacting particles on scale-free networks. *Physical Review E*, *74*(6), Article 066113.

Alemu, A., Shiferaw, Y., Addis, Z., Mathewos, B., & Birhan, W. (2013). Effect of malaria on HIV/AIDS transmission and progression. *Parasites & Vectors*, *6*(1), 1–8.

Arcede, J. P., Caga-Anan, R. L., Mentuda, C. Q., & Mammeri, Y. (2020). Accounting for symptomatic and asymptomatic in a SEIR-type model of COVID-19. *Mathematical Modelling of Natural Phenomena*, *15*, 34.

Arzt, J., Fish, I. H., Bertram, M. R., Smoliga, G. R., Hartwig, E. J., Pauszek, S. J., et al. (2021). Simultaneous and staggered foot-and-mouth disease virus coinfection of cattle. *Journal of Virology*, *95*(24), e01650–21.

Bailey, N. T., et al. (1975). *The mathematical theory of infectious diseases and its applications*. Bucks, U.K.: Charles Griffin & Company Ltd.

Berman, A., & Plemmons, R. J. (1994). *Nonnegative matrices in the mathematical sciences*. SIAM.

Bernoulli, D. (1760). Essai d'une nouvelle analyse de la mortalité causée par la petite vérole et des avantages de l'inoculation pour la prévenir. *Histoire de l'Academic Royale des Sciences (Paris) Avec les Mémoires des Mathematique & et Physique and Mémoires*, 1–45.

Beutel, A., Prakash, B. A., Rosenfeld, R., & Faloutsos, C. (2012). Interacting viruses in networks: Can both survive? In *Proceedings of the 18th ACM SIGKDD international conference on knowledge discovery and data mining* (pp. 426–434). ACM.

Bhat, S., James, J., Sadeyen, J.-R., Mahmood, S., Everest, H. J., Chang, P., et al. (2022). Coinfection of chickens with H9N2 and H7N9 avian influenza viruses leads to emergence of reassortant H9N9 virus with increased fitness for poultry and a zoonotic potential. *Journal of Virology*, *96*(5), e01856–21.

Briat, C. (2017). Sign properties of metzler matrices with applications. *Linear Algebra and its Applications*, *515*, 53–86.

Castillo-Chavez, C., Hethcote, H. W., Andreasen, V., Levin, S. A., & Liu, W. M. (1989). Epidemiological models with age structure, proportionate mixing, and cross-immunity. *Journal of Mathematical Biology*, *27*(3), 233–258.

Chen, L., Ghanbarnejad, F., Cai, W., & Grassberger, P. (2013). Outbreaks of coinfections: The critical role of cooperativity. *EPL (Europhysics Letters)*, *104*(5), 50001.

Chu, C.-J., & Lee, S.-D. (2008). Hepatitis B virus/Hepatitis C virus coinfection: Epidemiology, clinical features, viral interactions and treatment. *Journal of Gastroenterology and Hepatology*, *23*(4), 512–520.

Creighton, S., Tenant-Flowers, M., Taylor, C. B., Miller, R., & Low, N. (2003). Co-infection with gonorrhoea and chlamydia: How much is there and what does it mean? *International Journal of STD & AIDS*, *14*(2), 109–113.

de Souza, A. J. S., Gomes-Gouvêa, M. S., Soares, M. d. C. P., Pinho, J. R. R., Malheiros, A. P., Carneiro, L. A., et al. (2012). HEV infection in swine from Eastern Brazilian Amazon: Evidence of co-infection by different subtypes. *Comparative Immunology, Microbiology and Infectious Diseases*, *35*(5), 477–485.

Dupont-Rouzeyrol, M., O'Connor, O., Calvez, E., Daures, M., John, M., Grangeon, J.-P., et al. (2015). Co-infection with Zika and Dengue viruses in 2 patients, New Caledonia, 2014. *Emerging Infectious Diseases*, *21*(2), 381.

Fall, A., Iggidr, A., Sallet, G., & Tewa, J. J. (2007). Epidemiological models and Lyapunov functions. *Mathematical Modelling of Natural Phenomena*, *2*(1), 55–73.

Gracy, S., Paré, P. E., Liu, J., Sandberg, H., Beck, C. L., Johansson, K. H., et al. (2024). Modeling and analysis of a coupled SIS bi-virus model. arXiv preprint arXiv:2207.11414.

Hethcote, H. W. (2000). The mathematics of infectious diseases. *SIAM Review*, *42*(4), 599–653.

Hirsch, M. W. (1988). Stability and convergence in strongly monotone dynamical systems. *Journal fur die reine und angewandte Mathmatik*.

Janson, A., Gracy, S., Paré, P. E., Sandberg, H., & Johansson, K. H. (2020). Networked multi-virus spread with a shared resource: Analysis and mitigation strategies. arXiv preprint arXiv:2011.07569.
Kermack, W. O., & McKendrick, A. G. (1927). A contribution to the mathematical theory of epidemics. *Proceedings of the Royal Society of London. Series A, Containing Papers of a Mathematical and Physical Character*, *115*(772), 700–721.
Khalil, H. (2002). *Nonlinear systems*. Prentice Hall.
Khanafer, A., Başar, T., & Gharesifard, B. (2016). Stability of epidemic models over directed graphs: A positive systems approach. *Automatica*, *74*, 126–134.
Krauland, M. G., Galloway, D. D., Raviotta, J. M., Zimmerman, R. K., & Roberts, M. S. (2022). Impact of low rates of influenza on next-season influenza infections. *American Journal of Preventive Medicine*, *62*(4), 503–510.
Liu, J., Paré, P. E., Nedić, A., Tang, C. Y., Beck, C. L., & Başar, T. (2016). On the analysis of a continuous-time bi-virus model. In *Proceedings of the 55th IEEE conference on decision and control* (pp. 290–295).
Liu, J., Paré, P. E., Nedić, A., Tang, C. Y., Beck, C. L., & Başar, T. (2019). Analysis and control of a continuous-time bi-virus model. *IEEE Transactions on Automatic Control*, *64*(12), 4891–4906.
Matouk, A. (2020). Complex dynamics in susceptible-infected models for COVID-19 with multi-drug resistance. *Chaos, Solitons & Fractals*, *140*, Article 110257.
Mei, W., Mohagheghi, S., Zampieri, S., & Bullo, F. (2017). On the dynamics of deterministic epidemic propagation over networks. *Annual Reviews in Control*, *44*, 116–128.
Munster, V., & Fouchier, R. (2009). Avian influenza virus: Of virus and bird ecology. *Vaccine*, *27*(45), 6340–6344.
Newman, M. E., & Ferrario, C. R. (2013). Interacting epidemics and coinfection on contact networks. *PLoS One*, *8*(8), Article e71321.
Newman, M. E. J., Forrest, S., & Balthrop, J. (2002). Email networks and the spread of computer viruses. *Physical Review E*, *66*(3), Article 035101.
Norris, J. R. (1998). *Markov chains*. Cambridge University Press.
Paré, P. E., Beck, C. L., & Başar, T. (2020). Modeling, estimation, and analysis of epidemics over networks: An overview. *Annual Reviews in Control*, *50*, 345–360.
Paré, P. E., Liu, J., Beck, C. L., & Başar, T. (2018). A coupled bi-virus spread model in networked systems. In *Proceedings of the American control conference* (pp. 4414–4419).
Paré, P. E., Liu, J., Beck, C. L., Kirwan, B. E., & Başar, T. (2020). Analysis, estimation, and validation of discrete-time epidemic processes. *IEEE Transactions on Control Systems Technology*, *28*(1), 79–93.
Pawlowski, A., Jansson, M., Sköld, M., Rottenberg, M. E., & Källenius, G. (2012). Tuberculosis and HIV co-infection. *PLoS Pathogens*, *8*(2), Article e1002464.
Plemmons, R. J. (1977). M-matrix characterizations. I–nonsingular M-matrices. *Linear Algebra and its Applications*, *18*(2), 175–188.
Prakash, B. A., Beutel, A., Rosenfeld, R., & Faloutsos, C. (2012). Winner takes all: Competing viruses or ideas on fair-play networks. In *Proceedings of the 21st international conference on world wide web* (pp. 1037–1046).
Qu, Z. (2009). *Cooperative control of dynamical systems: Applications to autonomous vehicles*. Springer Science & Business Media.
Roberts, M. (2021). Covid: Woman aged 90 died with double variant infection. *BBC*.
Sahneh, F. D., & Scoglio, C. (2014). Competitive epidemic spreading over arbitrary multilayer networks. *Physical Review E*, *89*(6), Article 062817.
Santos, A., Moura, J. M. F., & Xavier, J. M. F. (2015). Bi-virus SIS epidemics over networks: Qualitative analysis. *IEEE Transactions on Network Science and Engineering*, [ISSN: 2327-4697] *2*(1), 17–29. http://dx.doi.org/10.1109/TNSE.2015.2406252.
Shuai, Z., & van den Driessche, P. (2013). Global stability of infectious disease models using Lyapunov functions. *SIAM Journal on Applied Mathematics*, *73*(4), 1513–1532.
Smith, H. L. (1988). Systems of ordinary differential equations which generate an order preserving flow. A survey of results. *SIAM Review*, *30*(1), 87–113.
Sontag, E. D. (2007). Monotone and near-monotone biochemical networks. *Systems and Synthetic Biology*, *1*(2), 59–87.
Souza, M., Wirth, F. R., & Shorten, R. N. (2017). A note on recursive Schur complements, block Hurwitz stability of Metzler matrices, and related results. *IEEE Transactions on Automatic Control*, *62*(8), 4167–4172.
Van Mieghem, P., Omic, J., & Kooij, R. (2009). Virus spread in networks. *IEEE/ACM Transactions on Networking*, *17*(1), 1–14.
Varga, R. (1999). Matrix iterative analysis. In *Springer series in computational mathematics*, Springer Berlin Heidelberg, ISBN: 9783540663218, URL https://books.google.se/books?id=U2XYs1DyKiYC.
Varga, R. S. (2009). Matrix properties and concepts. In *Matrix iterative analysis* (pp. 1–30). Springer.
Wang, Y., Chakrabarti, D., Wang, C., & Faloutsos, C. (2003). Epidemic spreading in real networks: An eigenvalue viewpoint. In *Proceedings of the 22nd international symposium on reliable distributed systems* (pp. 25–34).
Wang, L., & Sontag, E. D. (2006). A remark on singular perturbations of strongly monotone systems. In *Proceedings of the 45th IEEE conference on decision and control* (pp. 989–994). IEEE.
Wang, M., Wu, Q., Xu, W., Qiao, B., Wang, J., Zheng, H., et al. (2020). Clinical diagnosis of 8274 samples with 2019-novel coronavirus in Wuhan. MedRxiv.
Xu, S., Lu, W., & Zhan, Z. (2012). A stochastic model of multivirus dynamics. *IEEE Transactions on Dependable and Secure Computing*, *9*(1), 30–45.
Ye, M., Anderson, B. D., & Liu, J. (2022). Convergence and equilibria analysis of a networked bivirus epidemic model. *SIAM Journal on Control and Optimization*, *60*(2), S323–S346.
Zhang, C., Gracy, S., Başar, T., & Paré, P. E. (2022). A networked competitive multi-virus SIR model: Analysis and observability. *IFAC-PapersOnLine*, *55*(13), 13–18.
Zhao, L., Wang, Z.-C., & Ruan, S. (2020). Dynamics of a time-periodic two-strain SIS epidemic model with diffusion and latent period. *Nonlinear Analysis. Real World Applications*, *51*, Article 102966.

Sebin Gracy is an Assistant Professor in the Department of Electrical Engineering and Computer Science at South Dakota School of Mines and Technology. Previously, he was a Post-Doctoral Associate in the Department of Electrical and Computer Engineering at Rice University, and even prior to that he was a Post-Doctoral Researcher in the Division of Decision and Control Systems in the School of Electrical Engineering and Computer Science at KTH Royal Institute of Technology. He obtained his Ph.D. degree at Université Grenoble-Alpes in November, 2018. Prior to that, he obtained his M.S. and B.E. degrees in Electrical Engineering from the University of Colorado at Boulder and the University of Mumbai, in December, 2013 and June 2010, respectively. His research interests are in the realm of networked control systems. He is a member of the IEEE.

Philip E. Paré is the Rita Lane and Norma Fries Assistant Professor in the Elmore Family School of Electrical and Computer Engineering at Purdue University. He received his Ph.D. in Electrical and Computer Engineering from the University of Illinois at Urbana-Champaign in 2018, after which he went to KTH Royal Institute of Technology in Stockholm, Sweden to be a Post-Doctoral Scholar. He received his B.S. in Mathematics with University Honors and his M.S. in Computer Science from Brigham Young University in 2012 and 2014, respectively. He was a recipient of the NSF CAREER award in 2023, an inaugural Societal Impact Fellow at Purdue in 2021, and a 2023–2024 Teaching for Tomorrow Fellow at Purdue as well. His research focuses on networked control systems, namely modeling, analysis, and control of virus spread over networks.

Ji Liu received the B.S. degree in information engineering from Shanghai Jiao Tong University, Shanghai, China, in 2006, and the Ph.D. degree in electrical engineering from Yale University, New Haven, CT, USA, in 2013. He is currently an Assistant Professor in the Department of Electrical and Computer Engineering at Stony Brook University, Stony Brook, NY, USA. Prior to that, he was a Postdoctoral Research Associate at the Coordinated Science Laboratory, University of Illinois at Urbana-Champaign, Urbana, IL, USA, and the School of Electrical, Computer and Energy Engineering, Arizona State University, Tempe, AZ, USA. His current research interests include distributed control and optimization, distributed reinforcement learning, resilience of distributed algorithms, epidemic networks, social networks, and cyber–physical systems.

Henrik Sandberg is Professor at the Division of Decision and Control Systems, KTH Royal Institute of Technology, Stockholm, Sweden. He received the M.Sc. degree in engineering physics and the Ph.D. degree in automatic control from Lund University, Lund, Sweden, in 1999 and 2004, respectively. From 2005 to 2007, he was a Postdoctoral Scholar at the California Institute of Technology, Pasadena, USA. In 2013, he was a Visiting Scholar at the Laboratory for Information and Decision Systems (LIDS) at MIT, Cambridge, USA. He has also held visiting appointments at the Australian National University and the University of Melbourne, Australia. His current research interests include security of cyber–physical systems, power systems, model reduction, and fundamental limitations in control. Dr. Sandberg was a recipient of the Best Student Paper Award from the IEEE Conference on Decision and

Control in 2004, an Ingvar Carlsson Award from the Swedish Foundation for Strategic Research in 2007, and a Consolidator Grant from the Swedish Research Council in 2016. He has served on the editorial boards of IEEE Transactions on Automatic Control and the IFAC Journal Automatica. He is Fellow of the IEEE.

Carolyn L. Beck is currently Associate Head and Professor at the University of Illinois at Urbana-Champaign in Industrial and Systems Engineering, and has held visiting positions at KTH (Stockholm, Sweden), Stanford University and Lund University (Sweden). She is the President-Elect for the IEEE Control Systems Society (CSS), and also serves on the Board of Governors for the CSS. Carolyn is an IEEE Fellow and has been the recipient of a National Science Foundation CAREER Award, an Office of Naval Research Young Investigator Award, and local teaching honors. She received her Ph.D. from Caltech, her MS from Carnegie Mellon, and her BS from California State Polytechnic University, all in Electrical Engineering. Prior to her Ph.D., she worked as a Research and Development Engineer for Hewlett-Packard in Silicon Valley. Her research interests lie in the development of model approximation methods, network inference and aggregation, and distributed optimization and control, with applications to epidemic processes and energy networks.

Karl H. Johansson is Swedish Research Council Distinguished Professor in Electrical Engineering and Computer Science at KTH Royal Institute of Technology in Sweden and Founding Director of Digital Futures. He earned his M.Sc. degree in Electrical Engineering and Ph.D. in Automatic Control from Lund University. He has held visiting positions at UC Berkeley, Caltech, NTU and other prestigious institutions. His research interests focus on networked control systems and cyber–physical systems with applications in transportation, energy, and automation networks. For his scientific contributions, he has received numerous best paper awards and various distinctions from IEEE, IFAC, and other organizations. He has been awarded Distinguished Professor by the Swedish Research Council, Wallenberg Scholar by the Knut and Alice Wallenberg Foundation, Future Research Leader by the Swedish Foundation for Strategic Research. He has also received the triennial IFAC Young Author Prize and IEEE CSS Distinguished Lecturer. He is the recipient of the 2024 IEEE CSS Hendrik W. Bode Lecture Prize. His extensive service to the academic community includes being President of the European Control Association, IEEE CSS Vice President Diversity, Outreach & Development, and Member of IEEE CSS Board of Governors and IFAC Council. He has served on the editorial boards of Automatica, IEEE TAC, IEEE TCNS and many other journals. He has also been a member of the Swedish Scientific Council for Natural Sciences and Engineering Sciences. He is Fellow of both the IEEE and the Royal Swedish Academy of Engineering Sciences.

Tamer Başar has been with the University of Illinois Urbana-Champaign since 1981, where he is currently Swanlund Endowed Chair Emeritus and Center for Advanced Study (CAS) Professor Emeritus of Electrical and Computer Engineering, with also affiliations with the Coordinated Science Laboratory, Information Trust Institute, and Mechanical Science and Engineering. At Illinois, he has also served as Director of CAS (2014–2020), Interim Dean of Engineering (2018), and Interim Director of the Beckman Institute (2008–2010). He received B.S.E.E. from Robert College, Istanbul, and M.S., M.Phil, and Ph.D. from Yale University, from which he received in 2021 the Wilbur Cross Medal. He is a member of the US National Academy of Engineering, Fellow of the American Academy of Arts and Sciences, and Fellow of IEEE, IFAC, SIAM, and AAIA. He has served as president of IEEE CSS (Control Systems Society), ISDG (International Society of Dynamic Games), and AACC (American Automatic Control Council). He has received several awards and recognitions over the years, including the highest awards of IEEE CSS, IFAC, AACC, and ISDG, the IEEE Control Systems Award, and a number of international honorary doctorates and professorships. He has over 1000 publications in systems, control, communications, optimization, networks, and dynamic games, including books on non-cooperative dynamic game theory, robust control, network security, wireless and communication networks, and stochastic networked control. He was the Editor-in-Chief of Automatica between 2004 and 2014, and is currently editor of several book series. His current research interests include stochastic teams, games, and networks; multi-agent systems and learning; data-driven distributed optimization; epidemics modeling and control over networks; strategic information transmission, spread of disinformation, and deception; security and trust; energy systems; and cyber–physical systems.